



FINAL SCIENTIFIC REPORT

OTKA Project No. 101065.

Data model fusion for studying the combined effects of different land use and climate change scenarios on water regime and soil erosion



Principal investigator: Csilla Farkas
Project period: 01.02.2012 – 31.01.2017.
Institution: Institute for Soils Sciences and Agricultural Chemistry, CAR HAS and Eötvös Loránd University*, Budapest.
Participants: Zsófia Bakacsi, Györgyi Gelybó, Ágota Horel, Ilona Kása, Sándor Koós, József Kovács*, Péter László, Sándor Molnár, Imre Potyó and Eszter Tóth

Budapest, 2017.



Table of content

1. Introduction

2. Materials and Methods

- 2.1. Pilot catchments
- 2.2. Plot- scale measurements and monitoring
- 2.3. Catchment-scale measurements and monitoring
- 2.4. The modelling network
- 2.5. Linking the plot- and catchment scale models
- 2.6. Deriving site-specific future climate projections using the LARS-WG
- 2.7. Combined climate – and land use change scenario matrix

3. Results

- 3.1. Plot- and catchment-scale measurements
- 3.2. Plot-scale modelling of soil hydrological processes
- 3.3. Catchment-level modelling of runoff and sediment transport
- 3.4. The link between connectivity descriptors and model parameters
- 3.5. Results of the scenario analyses
- 3.6. Recommendations on climate smart solution

4. Discussion

- 4.1. The Project's achievements in the light of the expected deliverables

5. List of references



1. Introduction

Soil and freshwater quality of a region strongly determine (agro-)ecosystems functioning, ecosystem services and the quality of life in the area. Water regime and mass transport through the vadose zone and in surface watercourses have major effect on water quality and soil functioning. Erosion damages fertile soils and contributes to the sedimentation and pollution of lakes and rivers, thus, threatening agro- and natural ecosystem.

According to predictions, the frequency of extreme weather events will increase in the future (JRC 2009, Pongrácz et al. 2009). Considering the sometimes quite rapid, human induced changes in the landscape, the joint effect of land use and climate changes may lead to so far unknown hydrological situations. Hence, thorough knowledge of factors governing the water and mass transport in soil and water bodies at different scales is needed to understand and manage the functioning of terrestrial and freshwater ecosystems and to develop appropriate tools for mitigating the possible harmful effects of anthropogenic pressures and predicted climate change.

The Project accomplished aimed at i) integrating knowledge on plot- and catchment scale description of water and mass transport and ii) evaluating the combined effects of different land use and climate change scenarios on water regime and soil erosion. Our objectives, in particular, were:

- to improve our understanding on the effects of extreme hydrological situation on water regime and soil erosion for increasing preparedness and adaptation to foreseen land use and climate changes,
- to carry out field measurements on hydrological characteristics and to test advanced sensors for measuring the soil water balance elements,
- to construct a realistic scenario matrix using information on the forecasted changes in climate, land use and water management and to perform complex multi-scale scenario analyses in the pilot areas for reducing uncertainty in modelling results,
- to estimate erosion losses by applying the process-based INCA-SED dynamic model,
- to couple existing and newly obtained data as well as field- and catchment scale hydrological models for developing multi-level adaptation strategies that could contribute to reducing the vulnerability of terrestrial and hydrological ecosystems to extreme weather conditions and
- to formulate recommendations on monitoring, mitigation and adaptation measures.

The work was organised in four work packages. The relationship between the WP's is presented in Figure 1.

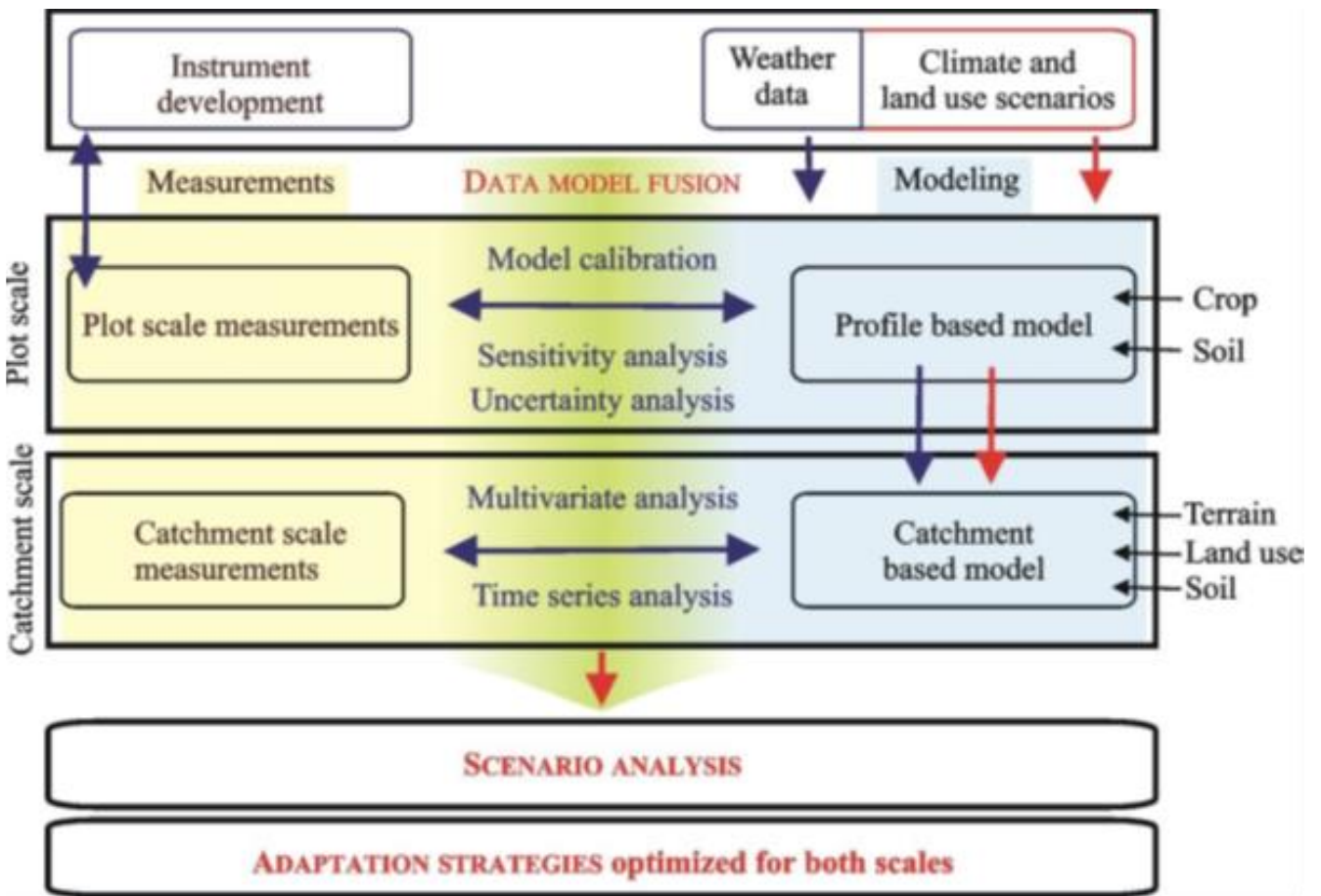


Figure 1. Conceptual structure and relations of the Project's activities

WP1 Data collection, measurements and monitoring; advanced data evaluation (yellow)

WP2 Data-model fusion (green) and models coupling (blue)

WP3 Scenario development and scenario analyses

WP4 Adaptation strategies optimised at field- and catchment scales



2. Materials and Methods

Table 1 gives an overview of the tasks, data sources and evaluation methods, used during the implementation of the Project.

Project goal, formulated in the Proposal	Time scale	Pilot area, involved	Data applied				Methods applied				Report chapters
			Already available	Measured (1 or a few times)	Monitored	Derived	Statistical analyses	GIS-based modelling	Mathematical modelling	Scenario analyses	
Related WP			WP1	WP1	WP1	WP3	WP1	WP2	WP2	WP3, WP4	
Studying the effects of extreme precipitation events on soil losses	event-based study (hourly resolution)	CR	land use data; basic soil data; DTM;	Soil properties	soil water content in different land use systems, runoff; turbidity; suspended sediment concentration		correlation between turbidity, suspended sediments				2.3; 3.1
Linking plot- and catchment scale models (connectivity study)	several years (daily resolution)	TR (full) and TR (in 6 sub-catchments)	Corine land use maps; soil maps; DTM;	Soil properties ;			advanced data evaluation	deriving connectivity parameters from maps	PERSIST, INCA		2.4; 2.5; 3.4
Scenario analyses on the effect of land use and climatic changes on water regime and sediment transport	several years (daily resolution)	TR; ER	Corine land use maps; soil maps; DTM; long-term daily water discharge; meteorological data	Soil properties; river bed properties at the outlet	soil water content in different land use systems, runoff; spended sediment concentration	climate change scenarios derived using the LARS Weather Generator			SWAP, PERSIST, INCA-SED	LARS WG	2.6; 2.7; 3.5

Table 1. Overview of the implementation of the Project’s goals – pilot area, data, methods

We faced different, sometimes unexpected problems during the accomplishment of the Project’s objectives. In the end of this Report, we give a short overview of the challenges faced, so that they could be avoided with higher probability in the future.

2.1. Pilot catchments

For representing the Lake Balaton watershed with its rather high erosional susceptibility, we selected three small representative catchments around the lake (Figure 2).

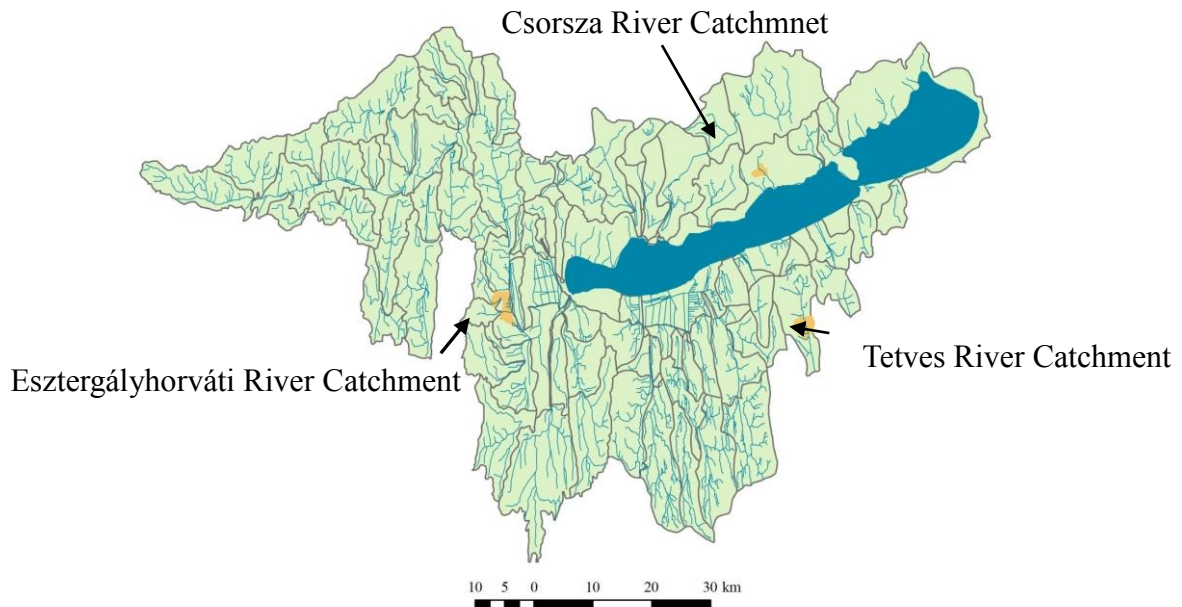


Figure 2. Lake Balaton watershed and location of the study cathments



The *Tetves River (TR) Catchment* (69 km²) lies on the southern part of the Balaton lake catchment (Figure 2), being one of the South-north oriented, 5-10 km wide meridional valleys typical for the area. The elevation of the area varies between 125 m and 301 m a.s.l., the average slope is 9.9 % (Szűcs 2012). The whole surface is covered mainly with carbonate rich eolian loess belonging to the loam, silty clay loam textural classes. On the bottom of the valleys, typically particles that contain more sand constitute the soil texture. The dominant soils types are Cambisols; notable clay illuviation occurs under forests where Luvisols could also occur (WRB 2006). The land use types are mostly forest, arable land, orchard and pasture, while the rest consists of scattered urban settlements and wetland. The long-term average (for the 1961-1990 period) annual temperature and precipitation amount in the Tetves River Catchment are 10.3°C and 650 mm, respectively (climatic information was retrieved from CRU CL v2.0 dataset; (New et al. 2002)).

The *Esztergályhorváti River (ER) Catchment* is located in the western part of the Lake Balaton watershed. Its length is approximately 9 km, with overall watershed area of 19 km². The typical soil types found in the area are brown forest soils (Dövényi, 2010). The land use types are mostly semi-natural forest, arable land, orchard and pasture. The average annual precipitation and temperature amount are in the catchment 650-690 mm yr⁻¹ and 10 °C, respectively.

The *Csorsza River (CR) Catchment* has an area of 21km² and river length of 8 km. The typical soil is forest soil and the mostly vineyard areas dominated by rendzina soils (Dövényi, 2010). The average annual precipitation and temperature are 10.2 °C and 580-680 mm yr⁻¹ (Table 2.)

Table 2. Main characteristics and yearly average meteorological data of study catchments and their surrounding areas.

Catchment	Area	Air temperature	Pot. evapo-transpiration	Precipitation sum	Wind speed	Groundwater depth
	km ²	°C	mm	mm	m/s	m
CR	21	10.3	750	580-680	3.0	2-4
TR	69	10.3	756	650	3.0	2-4
ER	19	9.9	800	630-680	2.7	2-4

The catchment-level studies (focusing on overall runoff and soil loss) were applied for the whole catchment, except the connectivity study, where the TR catchment was divided into 6 sub-catchments.

Concerning the plot-level studies, the measurements and model runs were performed for reference Hydrological Response Units (HRU's). The HRU's represent spatial units, homogeneous with respect to slope/elevation, soil cover and land use. They were selected by combining information available in the digital elevation model (DTM - slope), the Corine land use map (land use types - (European CORINE Land Cover 2000 spatial dataset (European Environment Agency) and the soil map (soil types) in order to establish plot-scale monitoring points. Thus, similar HRU's are considered to be similar in slope class, land use and soil type. The representative HRU land use types for the three catchments and are presented in Table 3.



Table 3. Characteristic land use classes in the pilot catchments

Catchment	HRU Land use classes (%)			
	Arable	Forest	Orchard	Pasture
TR	44	38	9	9
ER	49	42	3	6
CR	20	35	10	35

2.2. Plot- scale measurements and monitoring

At each HRU, the soil cover was analysed by collecting disturbed and undisturbed soil samples in three replicates from three different soil layers (at 15, 40 and 70 cm depth). From the disturbed samples, basic soil properties and the soil texture were determined. The undisturbed, 100 cm³ soil cores were used to measure the soil hydraulic properties – the soil water retention curve and saturated hydraulic conductivity. Table 4 demonstrates the soil properties, measured in the topsoil of the reference soil profiles in the CR catchment.

Table 4. Soil properties, measured in the 2-10 cm layer of the reference soil profiles in the CR watershed

Land use / Reference profile coordinates	Soil texture (3 fractions, MSZ-08-0205:1978)			pH (KCl)	CaCO ₃ %	EC 2,5 mS/cm	Humus %	HASL m	TSW %
	Sand %	Loam %	Clay %						
	Wineyard	12,1	36,2						
EOV: 546589, 175606	±1,3	±2,7	±2,7	±0,0	±6,1	±0,0	±0,5		±4,6
Arable land	10,4	44,8	44,8	7,1	18,1	0,25	1,9	220,1	55,2
EOV: 546052, 176715	±0,8	±1,1	±0,3	±0,0	±1,0	±0,0	±0,1		±6,28
Grass	22,7	39,85	37,5	5,8	0,0	0,28	3,8	282,3	56,8
EOV: 547173, 1767120	±0,8	±2,8	±2,3	±0,34		±0,1	±0,6		±3,0
Forest	15,9	55,0	29,2	5,4	0,0	0,23	3,9	284,4	59,5
EOV: 547150, 1767177	±0,3	±0,5	±0,3	±0,3		±0,1	±0,2		±3,6

HASL – Height above Sea Level; TSW – Soil water content at saturation, v%

The measured soil hydraulic properties are the key soil input data for the mathematical models. However, the models can not handle discrete data, therefore they require continuous (soil water retention and hydraulic conductivity) functions. We used the RETC software (<https://www.pc-progress.com/en/Default.aspx?retc>) to derive the Van-Genuchten – Mualem parameters representing the analytical forms of the soil hydraulic functions.



Soil temperature and soil water content probes were installed in selected reference HRU's. The soil water sensors were preliminary calibrated for the study sites. We used Decagon 5TM type sensors, connected to Decagon EM50 data loggers. The data were registered with hourly (at TR and ER for studies in daily resolution) and 10-minute resolution (at CR, for event-based investigations). The sensors were placed in three soil layers, representing the topsoil (0-20 cm), and the 20-60 and 60-100 cm layers. In some cases, no probes could be placed in the deepest soil layer.

For the event-based studies at the CR watershed, a Decagon ECH2O Rain sensor (model ECRN-50) was installed nearby the wine yard at 2 m height for registering the amount of rainfall with an accuracy of 1 mm. Further, simple plastic rain gauges were placed next to the soil water content probes in the grass, arable land, forest and orchards.

The rainfall data, together with other meteorological data were used as driving input variables for the mathematical models. The measured soil properties (and the derived Van-Genuchten – Mualem parameters) were used when parameterising the models for the study sites.

The soil water content data series were used as reference data to calibrate the SWAT plot-level soil hydraulic model to the reference HRU's.

2.3. Catchment- scale measurements and monitoring

Water discharge data (either received from responsible authorities or measured by the Team) were collected in daily resolution from the outlet points of the three pilot catchments, and used further as reference data for calibrating the PERSiST hydrological model and the hydrological routine of the INCA-P model.

Besides discharge measurements, water samples were collected manually from the studied rivers nearby the outlet first in weekly, later in daily resolution. The samples were analysed in the laboratory for suspended sediment content using vacuum filtration with 0.45 μm filter papers. Data on suspended sediment concentration were further used as reference data for calibrating the sediment transport (erosion) routine of the INCA-P model.

In 2015, a device for measuring turbidity was purchased. Turbidity measurements were performed at the outlet of the three pilot catchment, using a turbidity sensor connected to a ProDSS type YSI instrument. The instrument was pre-calibrated on standard solutions with known turbidity of 0, 10 and 1000 FNU ((Formazin Nephelometric Unit, Sigma–Aldrich). The FNU is the measure of turbidity, which is highly correlated with the suspended sediment concentration in waters.

Additionally, campaign measurements were carried out in the CR outlet to study the effect of extreme precipitation events on soil loss and suspended sediment concentration. The campaign measurements consisted of i) more frequent collection of water samples from the stream for measuring suspended sediment concentration and of ii) turbidity measurements.

Besides the daily water sampling at the Csorsza Patak monitoring station additional water samples were taken during high rainfall events, taking water samples hourly during the first six hours of the precipitation and every 2 hours during the next 42 hours (resulting in 24 samples per event).

2.4. The modelling network

The modelling network consisted of plot- and catchment level mathematical models, linked through i) common model parameters, ii) parameters that correlate with each other and iii) model outputs, providing input data for other models.



We used the SWAP (Soil, Water, Atmosphere and Plant) profile-based hydrological model to simulate the soil water regime of the selected HRU's at plot scale.

Further, two catchment level hydrological models - namely the PERSiST rainfall-runoff model and the hydrological routine of the INCA-P model - were used to describe the water pathways, the runoff within the pilot catchments and to evaluate the discharge at the catchment's outlet.

The model network is forced i) by daily meteorological data series for calibration and ii) by two climate scenarios, derived using the LARS Weather Generator for scenario analyses.

Plot-scale model: SWAP

The schematic description of the SWAP model in relation to volume balance parameters for soil, plant and environment is shown in Fig. 3. The model contains five sub-models of METEO, CROP, SOIL, IRRIGATION, and TIMER. Each sub-model receives the related input data and analyses it and sends the results to the main program. In sub-model SOIL, SWAP employs Richards' equation for soil water movement. Due to its physical bases, the Richards' equation allows the use of soil hydraulic functions and simulation of all kind of scenario analysis. The soil hydraulic functions are described by the analytical expressions of Van-Genuchten – Mualem or by tabular values. Root water extraction at various soil depths is calculated from potential transpiration, root length density and possible reductions due to wet, dry, or saline conditions.

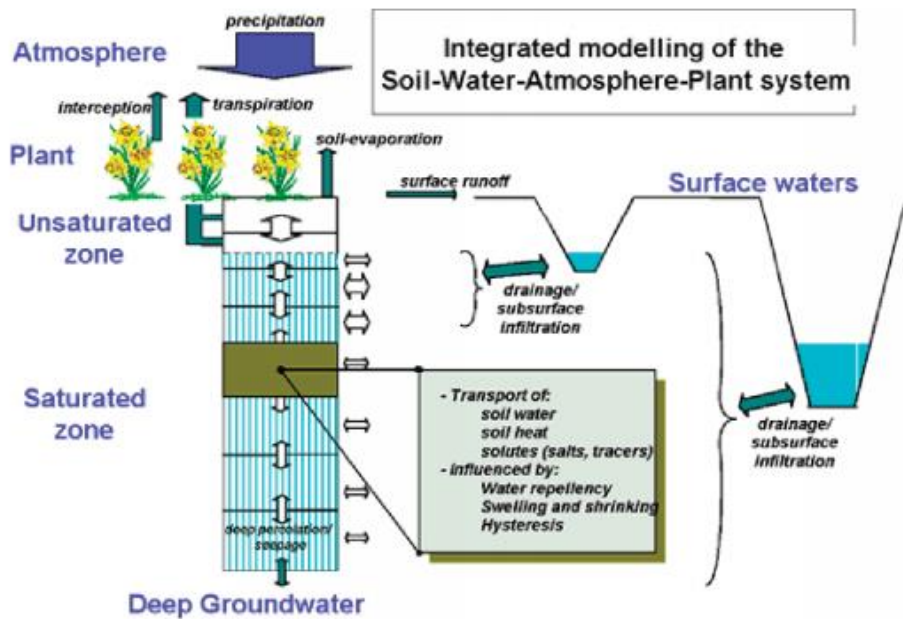


Figure 3. A schematized overview of the modelled system in the SWAP model

Catchment level models: PERSiST and INCA-P

We parameterized, calibrated and coupled the PERSiST (the Precipitation, Evapotranspiration and Runoff Simulator for Solute Transport) and the erosion module of the INCA-P (INtegrated CATCHment) models to simulate runoff and sediment transport in the Tetves River and Esztergályhorváti River Catchments (TR and ER Catchments).



The PERSiST model, developed at the Swedish Agricultural University is designed for simulating catchment hydrology, especially projecting possible future effects of climate or land use change on runoff and catchment water storage and generating hydrologic inputs for INCA model family (Futter, 2014).

The INCA-P model was designed at the Reading University, UK. This is a dynamic, process-based, daily-time step model simulating sediment delivery and designed to investigate the factors controlling phosphorus transformation and sediment transport processes (Whitehead et al., 1998a,b; Wade et al., 2002a.). The model has two main parts: (i) the land-phase delivery model which simulates the hydraulic and sediment generation and transport processes on the land, and (ii) the in-stream compartment that considers the processes and storage within the river segments (Fig. 4). The conceptual model that forms the basis of the numerical and computational sedimentation modul of INCA-P is presented on Fig. 5. (Lazar et al 2007). In this Project the hydrological and erosion modules of the INCA-P were applied.

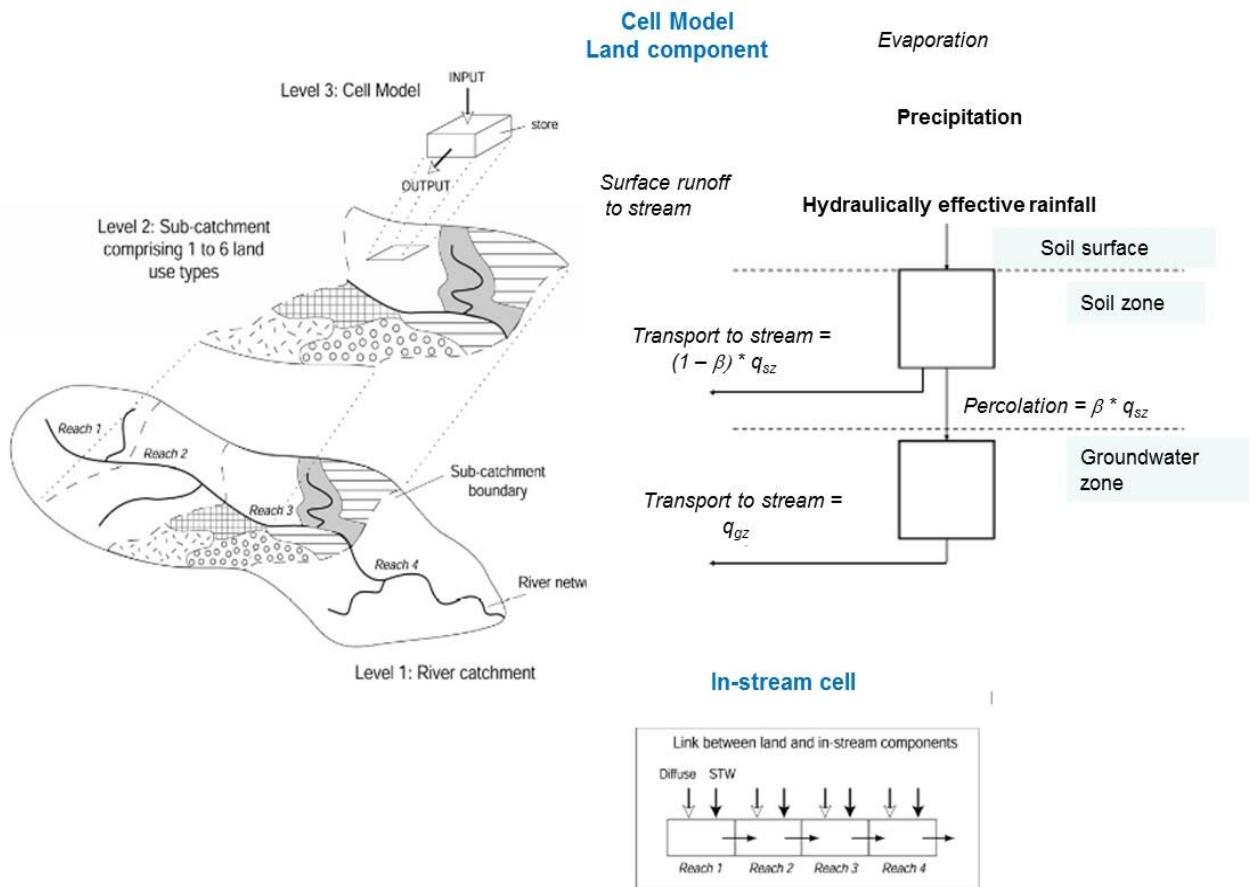


Figure 4. The hydrological routine of the INCA-P model

Being semi-distributed models, PERSiST and INCA-P share a common concept of representing a catchment as different combinations of landscape units or hydrological response unit (HRU). The HRUs consist of areas that can be regarded similar with respect to their soil cover, land use and slope characteristics. In the semi-distributed model structure, the water and sediment transport from different response units and sub-catchments are modelled simultaneously and information come consecutively into a multi-reach river model (Whitehead 2007.).



The selected models have been developed to simulate both terrestrial and aquatic systems and used to model a wide range of catchments (Futter et al. 2014, Whitehead 1998).

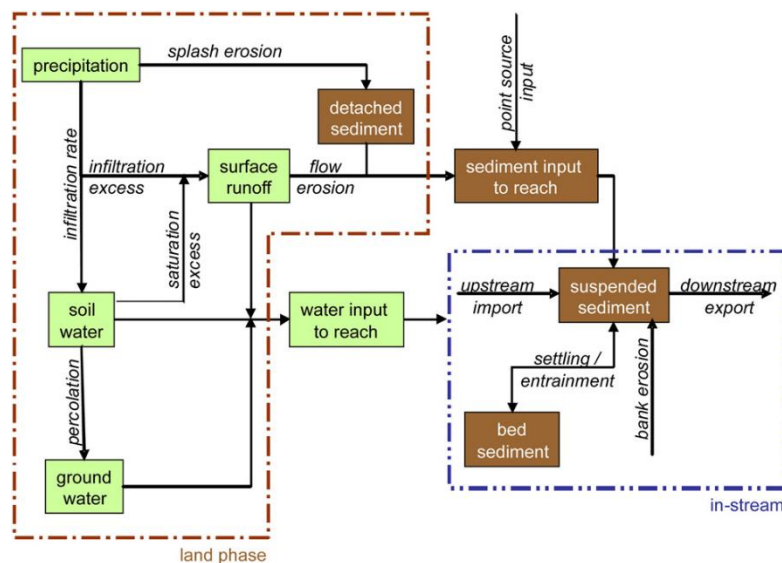


Figure 5. Conceptual model of the INCA-P erosion module (Lazar et. al. 2010)

Soil water content dynamics are not calculated directly in the INCA-P model; therefore, it requires soil moisture deficit (SMD) as an input from pre-processing of the data with PERSiST. The PERSiST model is capable of generating daily input time series for the INCA-P model consisting of hydrologically effective rainfall (HER) and SMD data in daily resolution. Hence, the two models have to be linked for running INCA-P, which means that the hydrological performance of the INCA-P model depends on how well the PERSiST model has been adapted to the catchment (Farkas et al. 2013).

Model parameterisation and calibration

The SWAP model was parameterized, using data registered at the reference HRU's. The soil parameters and initial conditions were set according to the measurements. As a relatively shallow soil profile was considered, free flux bottom boundary conditions were assumed. The crop parameters were set in accordance with the information about the crop cover.

The SWAT model is driven by daily meteorological data (daily minimum and maximum temperature, daily precipitation sum, wind speed, relative humidity and solar radiation). The input meteorological data files were prepared using data from Fonyód.

The model was run for the period, when measured soil water content data was available. The latter were used as reference data for model calibration.

The PERSiST and INCA-P was applied to the TR and the ER catchments (Figure 6). The TR catchment is a base flow-dominated system (BFI; 0.67), while the BFI is in case of ER Catchment is 0.17. The annual average BFI was obtained from a separation procedure using the local minimum method.

The reach lengths of the main river channel (19.0 and 9.3 km for TR and ER, respectively) were derived from the GIS database. Within the PERSiST and the INCA-P models, the following six hydrological response units were used: forest (slope: <12% and >12%) arable land (slope: <12% and >12%), orchard and pasture. The separation of arable land and forest into two PERSiST and



INCA land use categories was important to evaluate the effect of hillslope gradient on different soil management systems on run-off and sediment losses. The effects of slope gradient on soil loss and runoff were studied extensively, with the general conclusions that eroded materials and runoff increase with higher slope steepness. Minor land use types in the catchment (e.g. urban, wetland) were left out from the simulations and considered either as forest (wetland) or arable land (urban areas consisting mainly of scattered settlements).

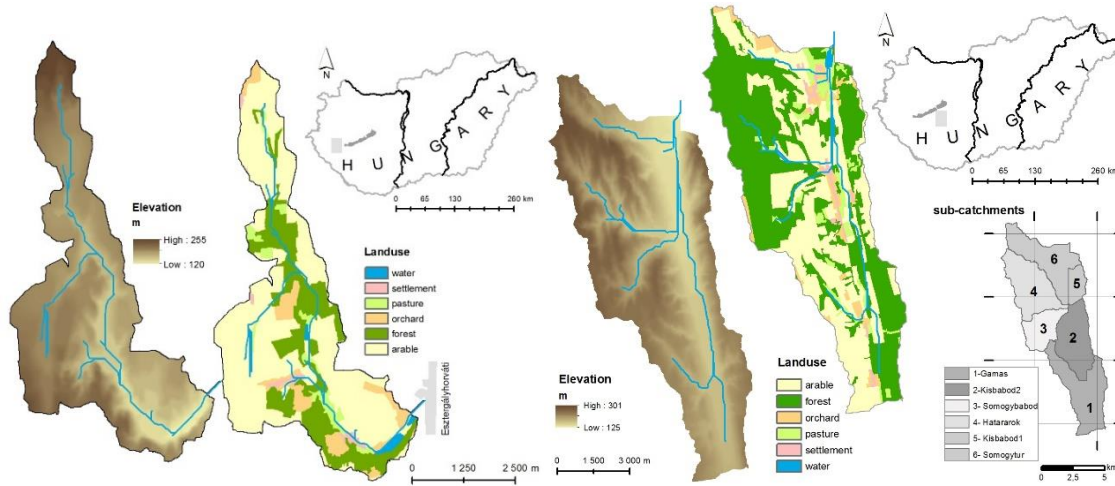


Figure 6. Land use and DTM of the TR and ER pilot watersheds

The hydrological modelling period was 1/1/2005-31/12/2016 in case of both study catchment. This period was split into calibration (2005-2009) and validation (2010-2016) periods. Suspended sediment concentrations were simulated for the period between 21/04/2015 and 31/12/2016 for TR Catchment and 21/05/2015-30/12/2016 for ER Catchment. The model calibration and validation were carried out by using the observed daily discharge and suspended sediment time-series. We calibrated the PERSiST and the INCA-P models manually by tuning model parameters to minimize the discrepancy between measured and simulated data.

We used different statistics to evaluate the goodness of fit of simulated values to observations. Simulated and observed discharge and sediment losses were compared using i) Pearson's correlation coefficient (R^2) and ii) the Nash–Sutcliffe model efficiency coefficient (NSE) (Nash & Sutcliffe, 1970), which are used to assess the predictive power of hydrological models. The NSE's value can range from $-\infty$ to 1. An efficiency of 1 corresponds to a perfect match of modelled values to observed data, 0 indicates that the model predictions are as accurate as the mean of the observed data, whereas efficiency less than zero occurs when the observed mean is a better than our estimates.



Table 5. Input and reference data, used for setting up and calibrating the PERSiST, INCA-P models and the LARS-WG models

Data	Description	Resolution	Type	Source
Meteorology	AP (2005-2016)	daily	input	Fonyód and Zalaapati station
	AT (2005-2016)	daily	input	
	AP (1970-1990)	daily	input for LARS-WG	CRU CL v2.0
	AT (1970-1990)	daily	input for LARS-WG	CRU CL v2.0
	HER	daily	Input for INCA	PERSIST output
Soil hydrology	SMD	daily		PERSIST output
Catchment geometry	Catchment area	-	input	Maps using GIS
Stream geometry	Length, average channel widths, slope	-	input	Maps using GIS
Land use	% of dominant land use types	yearly	input	CORIN Land cover
Discharge	Observed discharge at the outlets (TR-Visz and ER-Esztergályhorváti)	daily	reference	South- and West-Transdanubian Water Management Directorates
In stream suspended sediment concentrations	Samples taken at the outlets (TR-Visz and ER-Esztergályhorváti)	Approx. in every day	reference	MTA ATK TAKI dataset

AP and AT stand for annual precipitation and temperature, respectively.

2.5. Linking the plot- and catchment scale models

By making efforts on coupling the plot- and catchment scale models, we aim at:

- Linking two different approaches of simulating the water flow within natural systems, namely the soil water balance calculations and watershed level runoff simulations. Traditional hydrological models are describing water movement through watersheds via three main pathways (surface, intermediate and groundwater flow), focusing on the discharges measured at the catchment outlet. These models tend to integrate the field-scale processes, and the soil and its hydrological properties are usually poorly represented. On the other hand, many activities and possible adaptation strategies for improving water retention are valid at field scale. By coupling field- and catchment level models we hope to use information obtained at profile- plot- field level from the plot-scale models to improve the land-use specific performance of the catchment level models.



- Deriving additional information for parametrizing and calibrating the plot- and catchment level models. Thus, if we have a well-calibrated parameter set at plot scale, we can adapt the joint parameters in the catchment level model.
- Providing additional input and reference data for the models from each other for improving model performance.
- Decreasing the uncertainty of model parameterization due to gaining information from different sources.

While implementing the Project, we used two different approaches to couple the plot- and catchment scale models. The first approach was based on using common parameter values and feeding the models (back and forward) with advance input and reference data.

The second approach is related to the connectivity theory, as we tried to derive connectivity characteristics related to model's parameters and to use them jointly in the plot- and watershed level models. This approach was tested on the Tetves River watershed.

2.5.1. Coupling the plot- and catchment level models within the model chain

The most widely used connections between the three models applied are schematized in Figure 7.

During the Project implementation, the following efforts were made to couple the plot- and catchment level models and benefit from the information and knowledge, implemented in the models:

- Introducing calibrated soil and crop parameters from SWAP in the PERSiST and INCA-P models
- Providing the INCA-P model with driving input variables, calculated by the PERSiST model
- Cross-checking the water balance elements, simulated by the different models (for example, testing, if the evapotranspiration values, calculated by the SWAP and PERSiST models are in agreement with each other; calculating the area specific runoff from the INCA-P results and comparing it with the surface runoff values, simulated by the SWAP model for a given surface unit etc.)

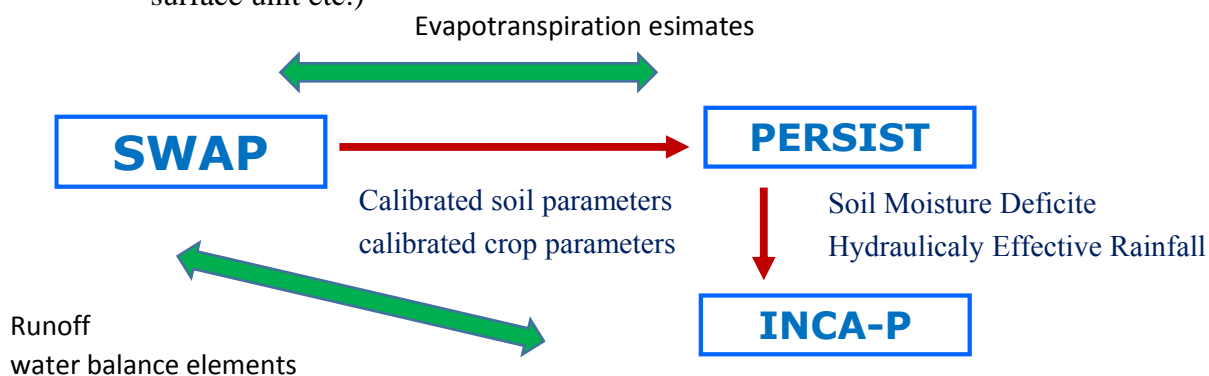


Figure 7. Data flow (red arrows) and cross-checking feedbacks (green) in the model chain



2.5.2. Linking the models via joint parameters derived using the connectivity theory (this work was carried out in collaboration with the Norwegian Institute for Bioeconomy Research (NIBIO) with contribution of Robert Barneveld)

A catchment's connectivity state is determined by morphometric and land use characteristics. We used a Digital Elevation Model (DEM) to assign the sub-catchments within the whole Tetves catchment and to derive connectivity parameters relevant for the area. The DEM was compiled based on 1:10 000 topographic contour maps, and had a 10 m spatial resolution (FÖMI). The characteristic land use types were defined in every cell of the 50 m × 50 m grid fitted to the Tetves catchment. The representative soil hydro-physical characteristics and vegetation properties, used in the models (see later) were defined according to the land use. Table 6 represents the main land use characteristics of the six sub-catchments, delineated within the TR watershed.

Table 6. The main physical characteristic of reaches and sub-catchments and proportion of land use classes within TR catchment

	1. Somogytúr (%)	2. Kisbabod 1 (%)	3. Határárok (%)	4. Somogybabod (%)	5. Kisbabod_2 (%)	6. Gamás (%)	Σ (%)
Arable	44	49	17	38	49	55	41
Forest	38	42	83	58	44	41	52
Orchard	9	3	-	4	3	-	4
Pasture	9	6	-	-	4	3	3
ΣArea (km ²)	14.1	11	14.4	7.4	5.5	15.6	68
Reach Lenght (m)	4940	4000	500	500	500	376 0	13400

As a next step, a number of connectivity-related discriminant catchment characteristics were derived for the entire catchment and the sub-catchments. Table 7 gives an overview of the descriptors. All calculations were carried out on a 10 by 10 regular grid.

With the exception of the altitude related parameters and the area and perimeter, all descriptors are presumed to affect the catchment's hydrological connectivity, either directly or indirectly. The shape parameters (Gravelius Index and radius) in combination with the drainage density will determine the maximum and average flow lengths. The combination of drainage density, catchment shape, slope and land use will determine the Index of Connectivity.

The last step was to evaluate the relationship between the key model parameters and the derived connectivity parameters. Multilinear regression functions for each of the hydrological calibration parameters of PERSiST and INCA models were derived by first identifying the catchment morphometric descriptor that had the highest Pearson correlation with that parameter. Since many of the morphometric characteristics are strongly correlated to each other, care was taken to avoid descriptors that are inter-dependent. The regression functions were processed with the Machine Learning in R (mlr) package in the R programming language (v. 3.0.2, The R Foundation for Statistical Computing, 2013). The scale-dependency of the fit of the regression functions was



investigated by determining the correlation between the relative error of the function and the area of the catchment.

Table 7. Catchment descriptive characteristics and their calculation.

Abbreviation	Descriptor	Calculation procedure
R_{min}	maximum radius (m)	The distance from the catchment centroid to the furthest point on the boundary.
R_{max}	minimum radius (m)	The distance from the catchment centroid to the closest point on the boundary.
A	surface area (m ²)	
P	perimeter (m)	
S	average slope (m m ⁻¹)	Average of the slope, calculated in the direction of the steepest neighbouring cell.
K_G	Gravelius Index (-)	$P (2 (\pi A)^{1/2})^{-1}$
L_{max}	maximum flow length (m)	Maximum distance a particle travels overland to the stream network, with deterministic 8 flow routing.
L_{av}	Average flow length (m)	Average of the flow length of all raster cells to the stream network.
H_{min}	Minimum elevation (m asl.)	
H_{max}	Maximum elevation (m asl.)	
H_{av}	Average elevation (m asl.)	
H_{range}	Elevation range (m)	
rA_{agri}	Ratio arable land	Ratio of arable land to the total surface area
DD	Drainage density (m ⁻¹)	Length of the combined streams divided by the area.
IC	Index of Connectivity (-)	The ratio of an upstream term that describes runoff generation, and a downstream term that quantifies the transport to the stream network.

2.6. Deriving site-specific future climate projections using the LARS Weather Generator

The IPCC climate scenarios, provided for further impact studies are the outcomes of Global or Regional Climate models (GCMs or RCMs), and the meteorological data series are given for the cross points of a grid. The spatial resolution of these data (the resolution of the grids) is insufficient for plot- and sub-catchment level studies.

To overcome this problem, we used a stochastic weather generator for deriving site-specific data series representing the future climatic conditions at the study catchments. The Long Ashton Research Station Weather Generator 5.0 (LARS-WG) is a stochastic weather generator developed by Semenov and Barrow (1997) for statistical downscaling. Several studies (such as Hashmi et al.,



2011) have compared the performance of LARS-WG with other statistical downscaling techniques and have concluded that LARS-WG can be adopted with confidence for climate change studies. LARS-WG version 5.0 includes climate scenarios based on 19 GCMs, which have been used in the IPCC 4AR Project (2007). The output data of LARS-WG are in the form of daily time-series for a suite of climate variables, namely, precipitation (mm), maximum and minimum temperature (°C), which are using inputs file for PERSiST and INCA-P.

In order to derive site-specific climate data series, the LARS-WG requires historical data series (for the reference years 1960-1990) from the study area. Further, it calculates a statistical matrix of differences between the measured data and those, incorporated in the LARS as historical data (1960-1990), valid for the grid points. This „matrix of differences” is used further to derive site-specific climate projections from the future climate projections, valid at the grid nearest grid points.

The Regional Climate Models, inbuilt in the LARS-WG and used in our study are given in Table 8. One can see, that there is a huge list of RCMs, the outcomes of which are incorporated in the Weather Generator – so the next question was to decide, which of the climate projections should be used in the Project for scenario analyses.

To make such a decision, the average air temperature and yearly precipitation sum of each of the RCMs from Table 8 were designed on a graph, the so-called thermoplviograms. These graphs allowed us to select the outstanding climate scenarios, and use them for running the mathematical models. Applying this approach we ensured, that all the possible future changes are represented in our study. The thermoplviograms for TR and ER catchments are given in Figure 7.

Table 8. Regional Climate Models, of which outputs are incorporated in the LARS-WG5.5

Models	Abbreviation	Resolution, Longitude/Latitude		Duration	Grid number
CCCMA CGCM3 T47 (medres)	CGMR	3.75	3.71	1850–2300	22
CNRM CM3	CNCM3	2.8125	2.79	1860–2299	33
LASG FGOALS-g1.0	FGOALS	2.8125	2.79	1850–2199	33
GISS AOM	GIAOM	4	3	1850–2100	27
UKMO HadCM3	HADCM3	3.75	2.5	1860–2199	27
UKMO HadGEM1	HADGEM	1.875	1.25	1860–2100	51
IPSL CM4	IPCM4	3.75	2.535	1860–2230	29
NIES MIROC3.2 hires	MIHR	1.125	1.1214	1900–2100	74
MPI-M ECHAM5-OM	MPEH5	1.88	1.87	1960–2200	32
NCAR CCSM3	NCCCSM	1.40625	1.400763	1890–2099	53
NCAR PCM	NCPCM	2.8125	2.79	1870–2099	33

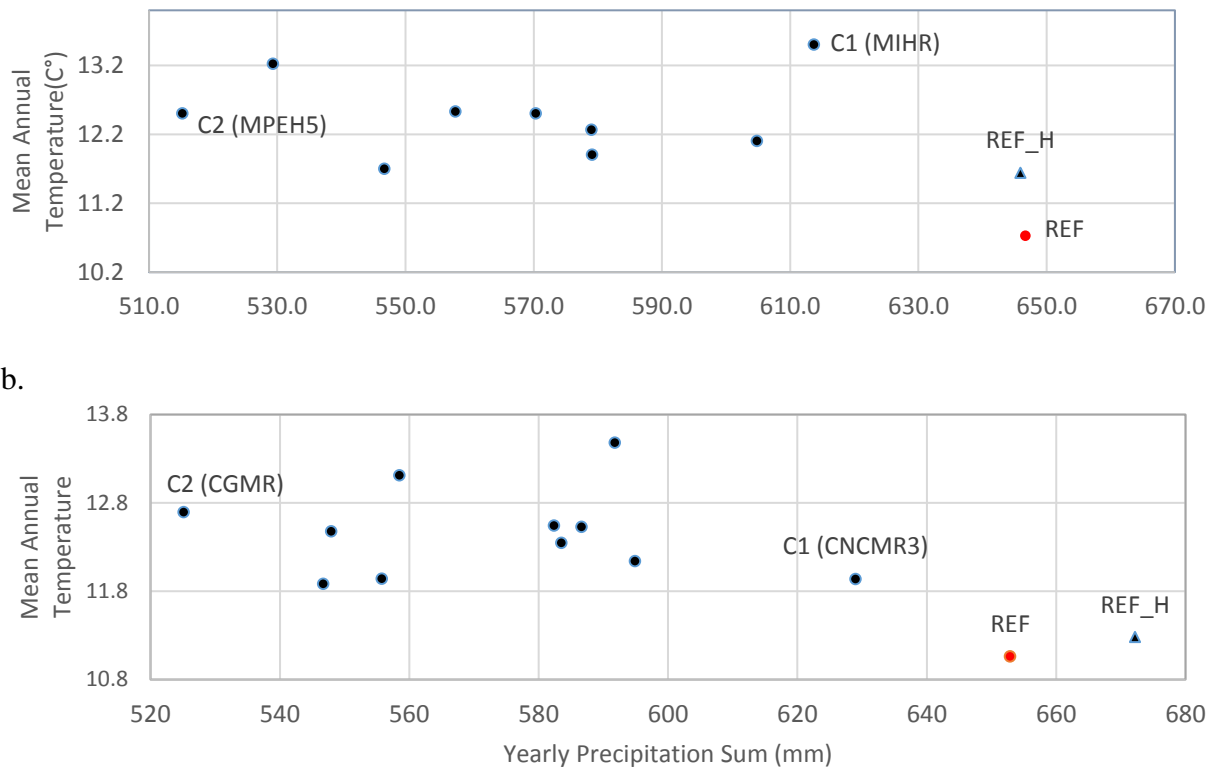


Figure 7.a-b. Thermopluviograms of the eleven regional climate models (IPPC 4AR, A1B, 2046-2065) and reference meteorological dataset (REF:1960-1990, REF_H:2005-2016) derived for the Tetves River Catchment (a) and Esztergályhoráti River Catchment (b)

All of the climate scenarios predicted increase in yearly average temperature and decrease in yearly average precipitation sum (Figure 7.) compared to the reference period. C2 -MPEH5 and -CGMR scenarios predict remarkable precipitation decrease during summer. (In this study the period from 2005 to 2016 was used as a reference, for modelling hydrological and sediment delivery, as the weather data used in the simulations belonged to this period. The projected trends in the future climate conditions might differ from those, where the reference period lasts from 1960 until 1990.

2.7. Combined climate – and land use change scenario matrix

Four management scenarios were considered to study the effects of human-induced land management changes on run-off and sediment transport processes. The PERSiST and INCA-P model were run for the calibration period with altered management options adjusting land phase parameters using the calibrated parameter set. The reference scenario (M0) represents current loadings from land-use. The M1 scenario represents applying winter cover crop on all arable land, which means permanent soil coverage all over the year. M2 scenario runs consider that 30% and 20% of forest will be converted into arable land for slopes under and above 12%, respectively. As for the M3 scenario, they show 30% reduction of arable land for areas with slopes under 12%, and 50% reduction of arable land for steep areas (slope above 12%), which are then converted to forest cover. Further, we also run the models with combinations of M2+M1 and M3+M1 scenarios.

The combined climate – land use change scenarios consisted of the combinations of the above described management scenarios and the climate change scenarios, selected using



thermopluviograms. Consequently, all the management scenarios (M0, M1, M2, M3 and M2+M1 and M3+M1) were forced by C1 (MIHR and CNCMR3) and C2 (MPEH5 and CGMR) climate scenarios.

The full overview of the scenario matrix, developed within the frames of the Project is given in Table 12 (sub-chapter 3.5).



3. Results

3.1. Plot- and catchment-scale measurements (examples)

A huge amount of data was collected and evaluated during the project. Hereby we just give some examples of how the data was used to achieve the Project's objectives.

Figure 8 demonstrates the measured soil water content dynamics in the different land use classes of the CR catchment in three different soil layers, as well as the measured precipitation amounts.

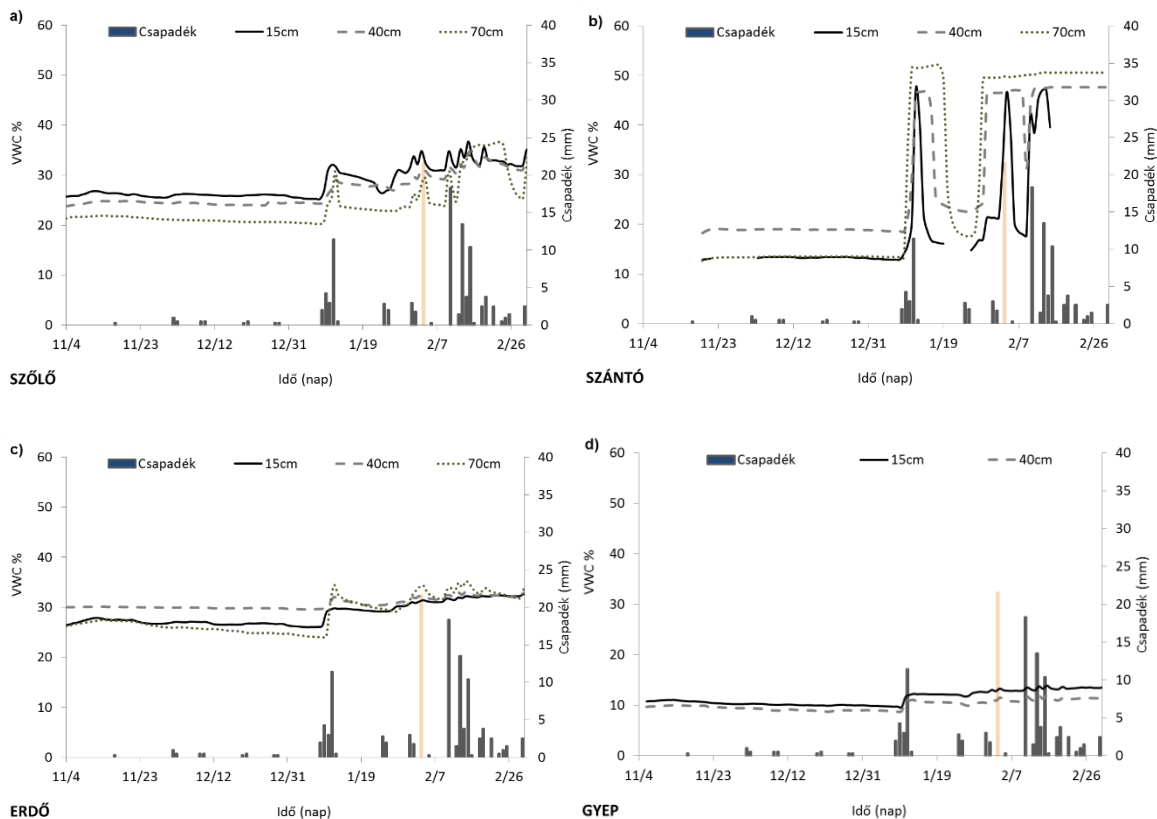


Figure 8.

Soil water content (VWC, in v%) and daily precipitation sum (Csapadék, mm) measured during the period between 04.11.2015 and 29-03-2016 in the different land use classes.

a) wine yard; b) arable land; c) forest; d) grassland

The driest conditions were detected in the forested areas and on grassland. In addition, the fluctuation of the soil water content was less expressed in these areas. Analysing the soil water regime (the possible dry or oversaturated periods) we can make assumptions on the differences between the runoff amounts from the different land use classes, and, consequently, get indirect information about the land use specific soil erosion conditions.

In Table 8. we present the Van Genuchten parameters, derived from undisturbed soil samples and further used as soil input data in the SWAP model.



Table 8. Soil water retention characteristics, measured in the TR watershed in two different land use classes and the corresponding Van-Genuchten parameters

soil water potential cm	TR_arable land			TR_forest		
	Measured water retention data					
	0-30	30-60	60-90	0-30	30-60	60-90
1.00	43.69	44.77	43.18	43.03	44.96	46.24
2.51	43.12	44.11	42.63	42.47	44.57	45.99
10.00	40.37	41.99	40.55	40.37	42.21	43.77
31.62	39.22	39.86	38.10	39.53	41.30	42.51
100.00	36.84	35.96	34.12	35.25	37.02	38.60
199.53	33.90	32.71	29.82	32.04	32.97	33.39
316.23	31.05	29.66	26.44	29.69	29.95	29.27
2511.89	17.64	20.58	18.00	19.82	18.93	17.59
15848.93	10.41	13.78	11.53	12.54	12.50	10.12
Derived Van-Genuchten parameters						
Theta_Sat	42.15	44.05	42.66	42.25	44.27	45.60
alpha	0.01	0.02	0.03	0.02	0.02	0.01
n	1.29	1.19	1.21	1.21	1.23	1.28
Theta-Res	0.02	0.03	0.01	0.03	0.03	0.01

Theta_Sat- Saturated soil water content (v%)

Alpha, n – fitting parameters (1/cm and “-“, correspondingly)

Theta-Res – residual soil water content (v%)

For all the three catchments, the suspended sediment concentrations (TSS) were compared with the turbidity measurement results aiming to find correlation between these two values so that the time-consuming TSS determination could be substituted with turbidity measurements in the future.

Suspended sediment concentrations, determined from collected water samples at the outlet of the three pilot watersheds are given in Figure 9. The statistical relationship between the TSS and FNU values is demonstrated in Figure 10.

We found that TSS and FNU values were well correlating at high TSS and FNU concentrations (Fig. 10), while only weak but still positive correlations were observed below 60 mg L⁻¹ TSS values (data not shown). The ER watershed didn't exhibited many high TSS concentrations during the investigated 2 years period, as the 97.2% of all samples presented a value below 60 mg L⁻¹, due to the fishing lakes prior to the water sampling site might cause sediment settling with water flow velocity decreases. Therefore, minimal suspended solid contamination were observed at the ER site even at high amount of rain events. We found the total of 1.1×10^5 mg L⁻¹ and 4.3×10^5 mg L⁻¹ TSS for TR (n=357) and CR (n=312), respectively for 2016 (when entire year was covered from January 1 through December 31) entering Lake Balaton, where X% of TSS were observed during or after heavier rainfalls (≥ 6 mm). At ER site we observed only 0.64×10^5 mg L⁻¹ TSS in 2016; however at this site we usually collected 5 samples per week (n=248); therefore this number is lower than actual TSS. We only observed weak correlation between suspended solid amount and water throughput/discharge volume (data not shown).

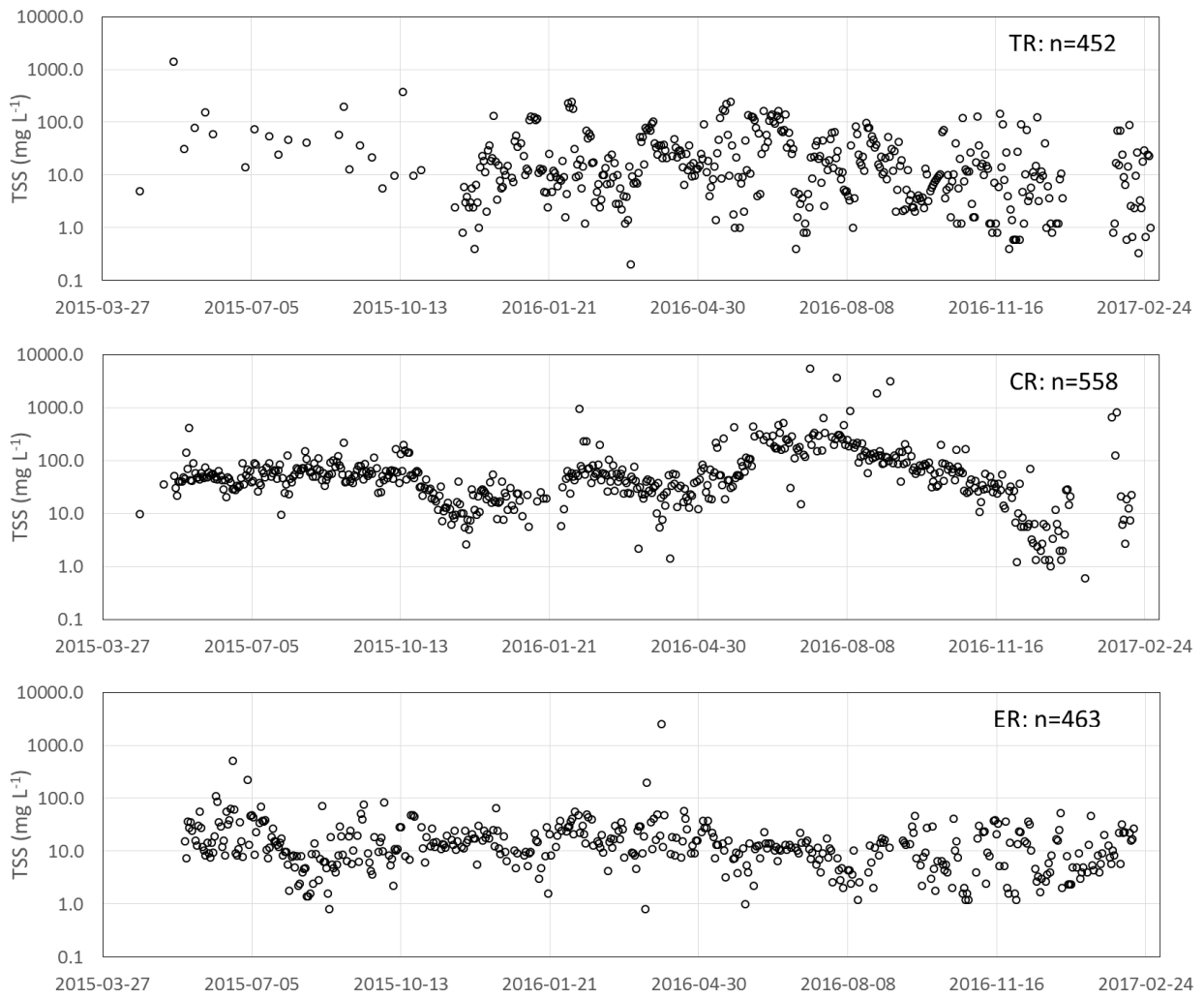


Figure 9. Water samples collected and analysed for TSS concentrations during 2015, 2016, and early 2017 at the three catchment outlets

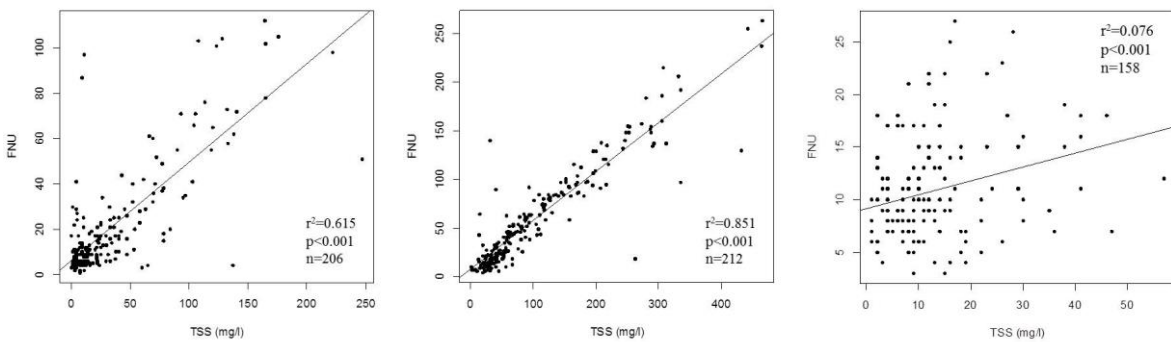


Figure 10. Linear regression analyses between total suspended solid (TSS) quantity and turbidity (FNU) values at a) TR catchment; b) CR catchment; and c) ER catchment.



3.2. Plot-scale modelling of soil hydrological processes

The calibration of the SWAP simulation model to the measured soil water content data was moderately successful for soil profiles, where the data series were long enough to perform model calibration. Despite of early installation of the soil water content probes, the measured soil water content dynamics data were not satisfactory.

The probes were often destroyed (stolen, disturbed by animals or agricultural machinery), or the records were unrealistic (probably due to root activity, soil cracking etc.).

For HRU's, where the data records were satisfactory the model calibration was moderately successful. The reason for that is the strong precipitation data dependency of the plot-scale model output. For catchment levels models, the processes are integrated over larger areas, and even if there are differences between the precipitation amounts, recorded at the meteorological station and really falling down in the catchment, the input data errors are more smoothed, than in case of the plot-scale models.

Figure 11 demonstrates the measured and simulated soil water content dynamics for the TR watershed for arable areas. Figure 12 shows the relationship between total amount of water in the upper 60 cm soil layer of the TR catchment under forest. The goodness-of-fit statistics are indicated in the graphs.

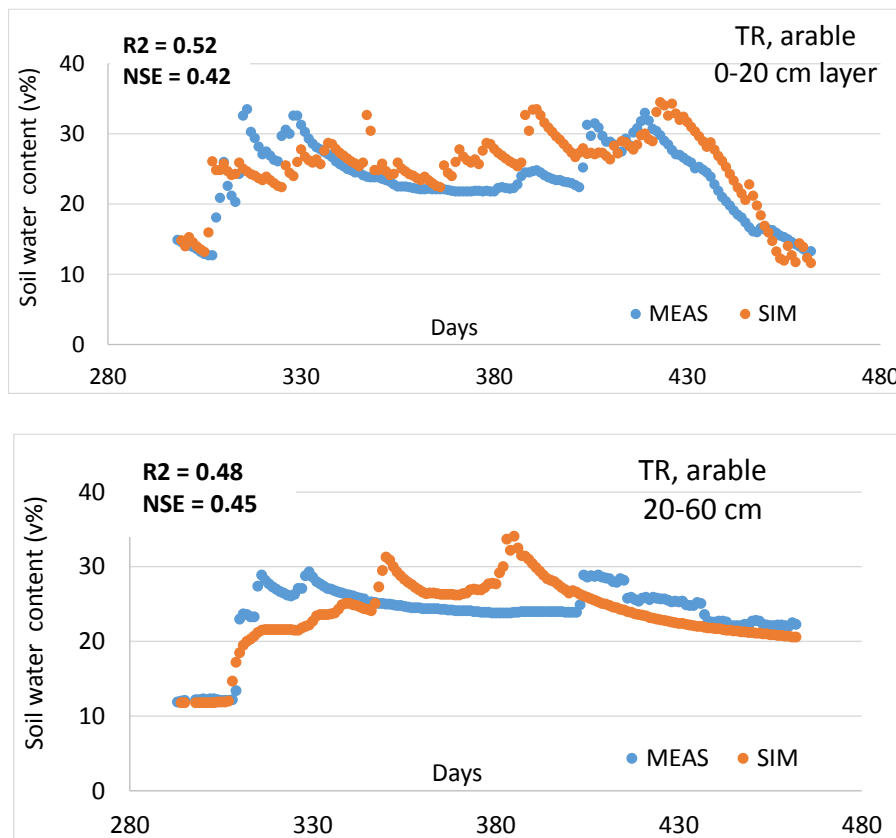


Figure 11. Measured and simulated using the SWAP model soil water content data for the arable land use area of the TR catchment

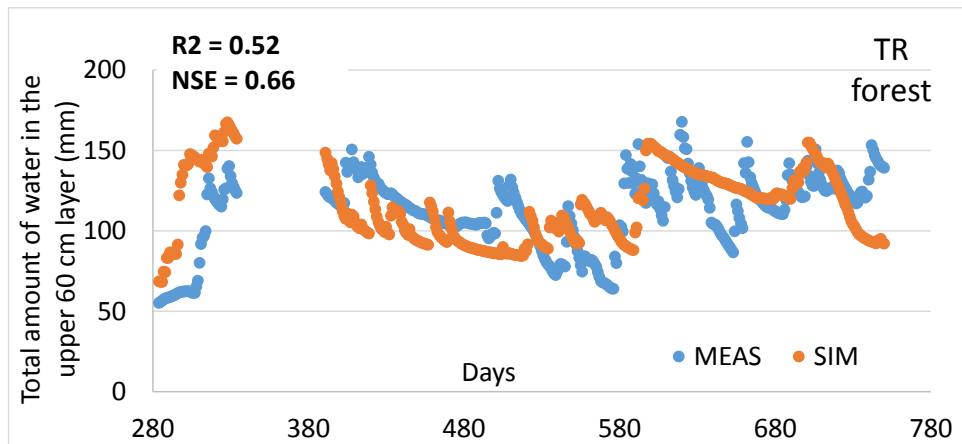


Figure 12. Measured and simulated using the SWAP model total amount of water in the upper 60 cm of the soil under the forested area of the TR catchment

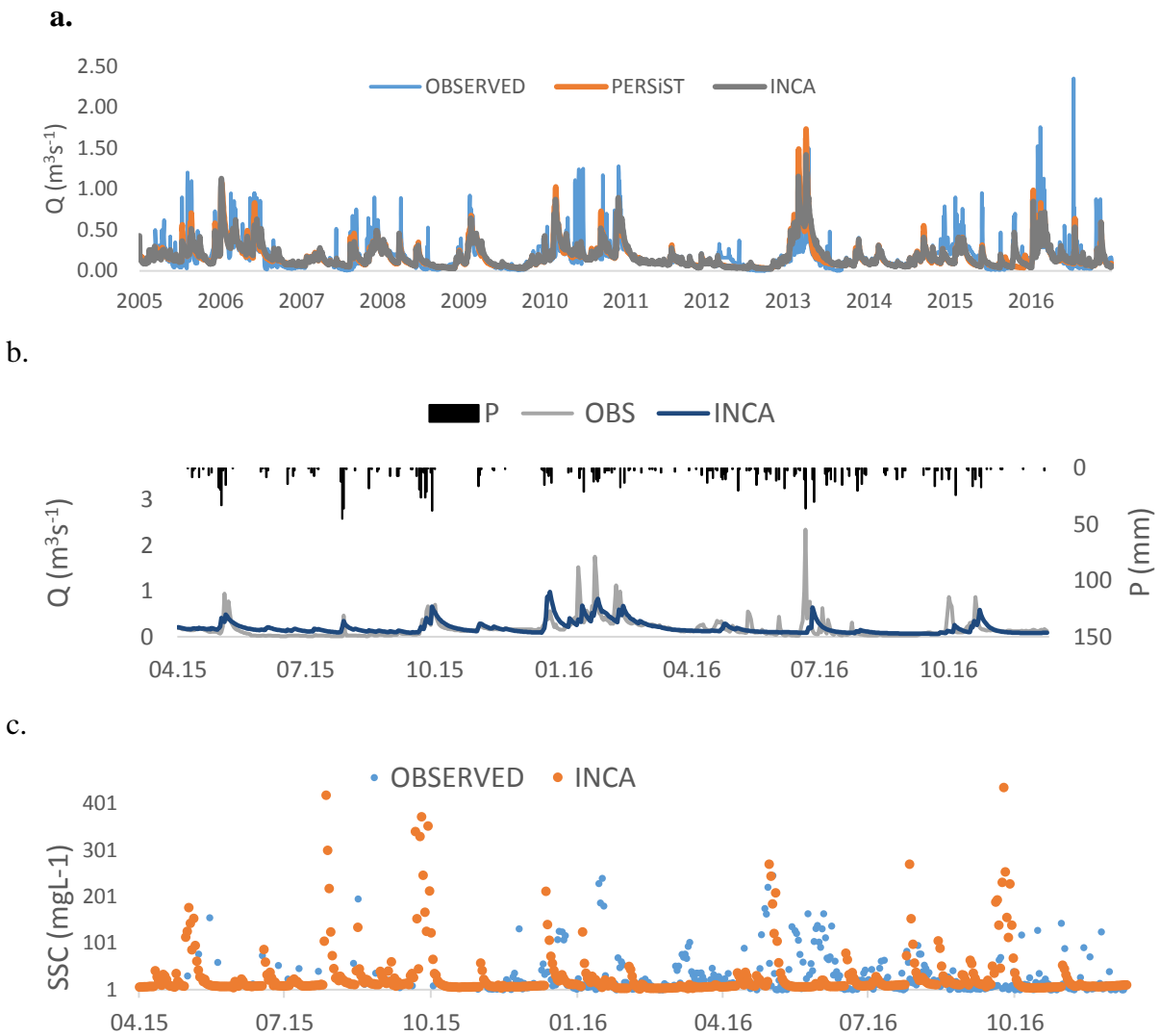
Note, that the total amount of water is an integrated characteristic compared to the soil water content of the individual soil layers, and as such, can be simulated with higher certainty. We obtained good statistics for this simulation, which indicates that the model might be not strong in simulating the redistribution of water between the soil layers, but can give satisfactory estimates of the total amount of water stored in the soil profile. In this case we can assume, that the model can give good estimate of the other water balance elements – surface runoff, evapotranspiration, deep percolation etc., therefore, the SWAP model can be used for providing parameters and water fluxes information in catchment-level studies.

3.3. Catchment-level modelling of runoff and sediment transport

We used the Pearson's correlation (R^2) and the Nash–Sutcliffe model efficiency index for untransformed (NSE) series for evaluating the performance of the the PERSiST and the INCA-P models (Table 9).

The simulated discharge values were evaluated on daily and monthly bases. The goodness-of-fit statistics were significantly better for on monthly base compared to the daily base in case of both catchment. On monthly based simulation result ranged between 0.23-0.92 (R^2) and 0.11-0.87 (NSE) and 0.3-0.69 (R^2) and 0.14-0.58 (NSE) for TR and ER catchments, respectively. These results were not surprising because daily values of discharge reflected individual extreme events that were more difficult to simulate (Farkas et al. 2013).

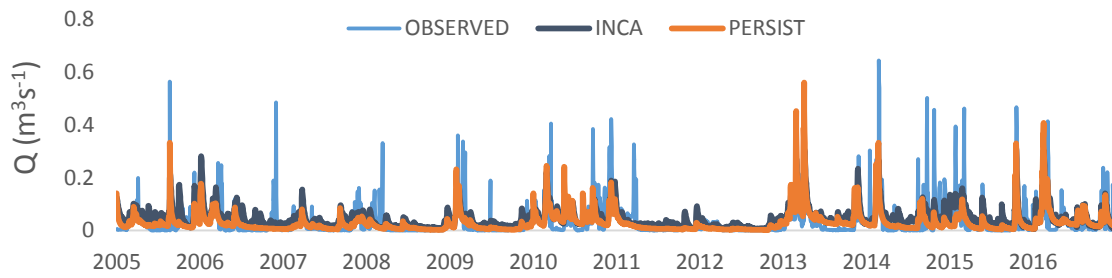
In general, the hydrographs of daily base simulations of discharge match the observed data relatively well, but model simulations show that both hydrological models underestimate high flow events (Figure 13.a-b), however the timing of the peaks were captured well. In general, the discrepancy between observed and simulated data was much higher in the validation period than in the calibration period in case of both the models, excluding INCA-P giving lower NSE and R^2 values in the calibration period for ER Catchment compared to the validation period.



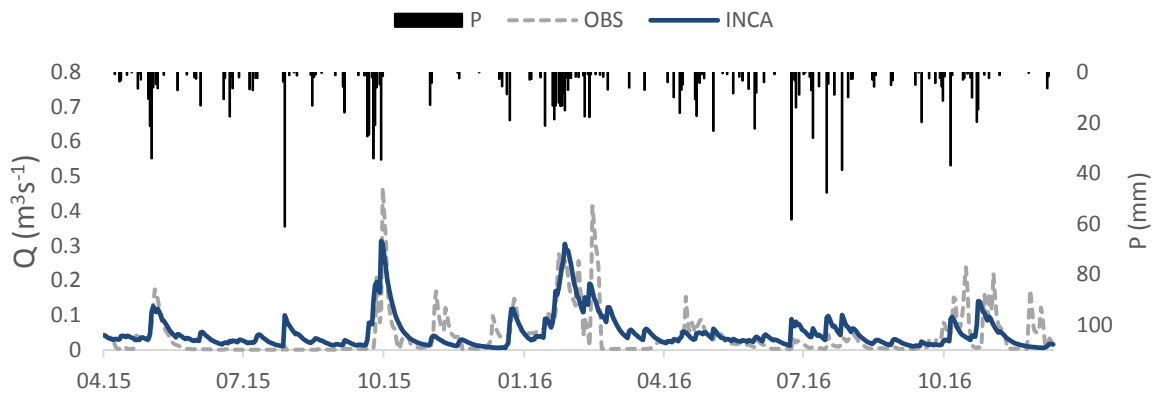
Figures 13. a-c. a, Measured and simulated water discharge by PERSiST and INCA-P for period 2005-2016, b, measured and simulated water discharge, precipitation for period 2015-2016. c. measured and simulated suspended sediment concentration for period 2015-2016 at the **Tetves River (TR)** catchment outlet,



a.



b.



c.

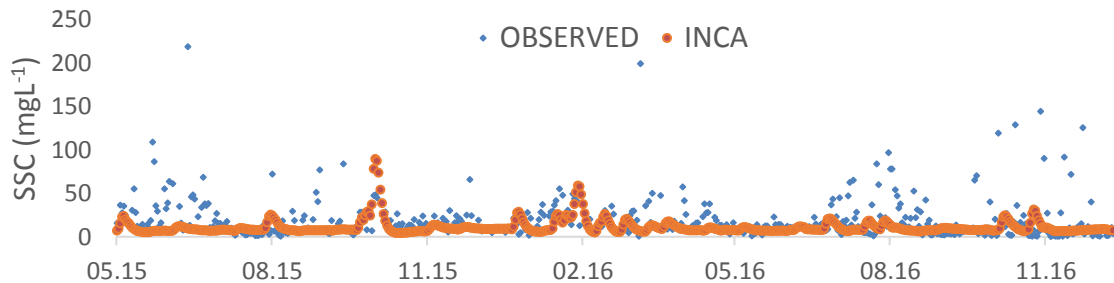


Figure 14. a-c. a, Measured and simulated water discharge by PERSiST and INCA-P for period 2005-2016, b, measured and simulated water discharge, precipitation for period 2015-2016. c. measured and simulated suspended sediment concentration for period 2015-2016 at the **Esztergályhorváti River (ER)** catchment outlet,



Table 9. Goodness-of-fit statistics for the PERSiST and INCA-P models

Catchment/ Time step	Discharge (Q)				Suspended Sediment (SSC)	
	R ² / NSE		R ² / NSE		R ² / NSE	
	Calibration (2005-2009)	Validation (2010-2016)	2015	2016	2015	2016
TR/Monthly INCA-P	0.81/0.80	0.51/0.35	0.91/0.87	0.5/0.35	0.83/0.83	0.23/0.11
TR/Monthly PERSiST	0.85/0.82	0.55/0.52	0.92/0.87	0.51/0.37	-	-
TR/Daily INCA-P	0.54/0.53	0.37/0.20	0.77/0.71	0.33/0.24	*Approx.. weekly	0.02/-0,3
TR/Daily PERSiST	0.62/0.59	0.34/0.31	0.8/0.72	0.37/0.25	-	-
ER/Monthly INCA-P	0.46/0.43	0.56/0.52	0.69/0.58	0.3/0.19	0.47/0.24	0.3/0.14
ER/Monthly PERSiST	0.51/0.5	0.48/0.44	0.67/0.58	0.29/0.2	-	-
ER/Daily INCA-P	0.23/0.22	0.37/0.36	0.57/0.5	0.17/0.1	0.26/0.03	0.1/-0.01
ER/Daily PERSiST	0.39/0.38	0.27/0.21	0.55/0.47	0.17/0.11	-	-

The observed and simulated sediment losses were in relatively good agreement in 2015 (Figure 13c., 14c.), 0.83 (R²) and 0.83 (NSE) for TR Catchment and 0.47 (R²) and 0.24 (NSE) for ER Catchment on monthly base (Table 8.). SSC simulations gave less satisfactory results in case of both study catchment in 2016, ranging between 0.11-0.3 (R², NSE). The simulated SSC values were evaluated on daily and monthly bases; the statistics were notably better when regarded on a monthly base (by comparing the measured and simulated total monthly losses) compared to the daily base on both catchment. The hydrological models did not simulate accurately some of the high flow events, but the average modelled flow is fitted satisfactory to the observed data. Accordingly, the “average” SSC are captured relatively well, whereas the extreme concentrations are not simulated adequately by the model. TR and ER are relatively small, fast reacting, flashy catchments and the model cannot satisfactory reproduce the flashy sediment response and great variability trends seen at the River Tetves and Esztergályhorváti. This can be related to the time resolution of the model, as a daily time step model might not be enough to describe the rapid reaction of small catchments to extreme weather events (Kása et al 2016). Another reason might be the consequence of using only one precipitation and soil moisture deficit time series for the entire catchment derived from PERSiST, whilst rainfall events could be extremely local. Simulation results demonstrate that actual peak value is difficult to model precisely and would require further calibration of the model with this calibration objective as the target (Jarritteel al 2005).

Jarrit and Lawrence (2006) pointed out to that differences between observed and simulated sediment concentrations may be the consequence of several factors, such as, not enough precise representation of sediment sources derived from river bank erosions or the coarse spatial structure of the hillslope component of the INCA model. Nevertheless, positive N-S values of ca. 0.3 on monthly base simulation are considered to be satisfactory (Moriassi et al. 2007).



The results of the sensitivity analyses are given in Table 10.

Table 10. Critical parameters for adjusting land-use specific sediment losses to the reference data

Hydrological parameters	Hydraulic parameters	Sediment parameters
T1-Direct runoff residence time	c4-V/Q linear multiplier	a1-Flow erosion multiplier
T2-Soil zone residence time	c5-V/Q power coefficient	a2-Flow erosion threshold
T3-Groundwater residence time		a3-Floe erosion coefficient
c1-Fraction of soil water to direct runoff		a4-Transport capacity multiplier
c2-Fraction of infiltration excess to direct runoff		a5-Transport capacity threshold
c3- Base-flow index		a6-Transport capacity coefficient
qsat-Threshold for soil zone flow to direct runoff		a7-Coeff. for boundary shear stress
I -Threshold infiltration rate		a8-Coeff. for bed entrainment rate

Figure 15 demonstrates the simulated land-use specific sediment losses from different sub-catchments, using the sub-catchment division as described in sub-chapter 2.5.2.

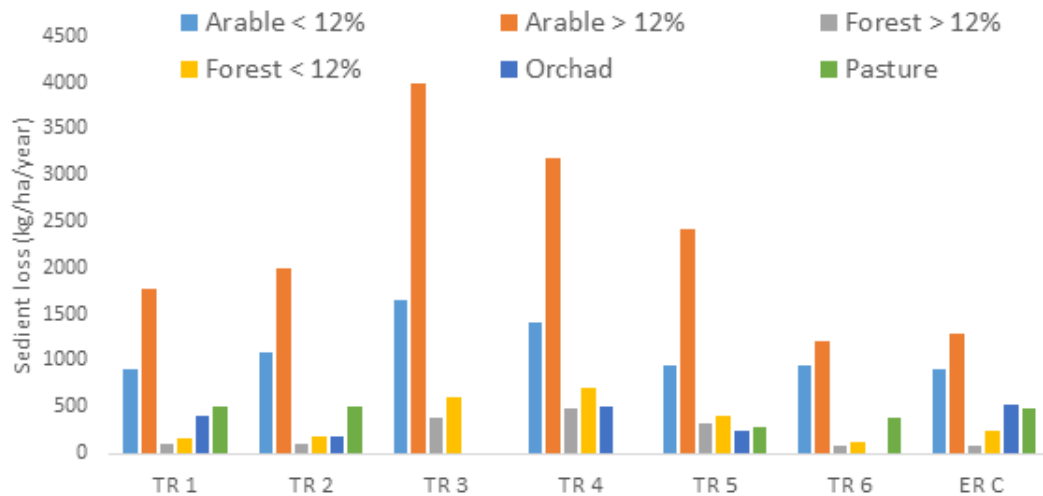


Figure 15. Simulated average land use specific sediment losses from the study catchments

Simulated sediment delivery concentrations to the River Tetves varies among land use types and relief conditions between 80- 4000 kg ha⁻¹ year⁻¹ (Figure 15). The average annual simulated sediment delivery for the entire Tetves catchment is 940 kg ha⁻¹ yr⁻¹ in the simulation period. These value are in relatively good agreement with the reported sediment delivery range for the Tetves Catchment that is 400-65000 kg ha⁻¹ yr⁻¹ (VITUKI, Dezsény, 1982, Jakab 2003, Szűcs, 2012). The INCA-P simulation's catchment average is 620 kg ha⁻¹ yr⁻¹ for ER Catchment. The predicted yearly sediment loss range varies between 88-1300 kg ha⁻¹ yr⁻¹ depending land use type and slope conditions. Szűcs (2012) reported sediment loss values 320 kg ha⁻¹ and 210 kg ha⁻¹ for 2004 and 2005, respectively on ER Catchment. Agriculture and semi-natural vegetation also plays an important role on erosion processes in both the catchments. TR and ER Catchment are prone to erosion, mostly on arable land over 12%. The simulation results indicate that the Tetves River catchment has three sub-catchments on the middle region, where the erosion is much higher, than on the other three. The middle part -represents the upper region with high relief and steeply slopes



(sub-catchments TR3, TR4, TR5) - deliver the highest amount of sediment to the river, mainly from arable land over 12%. The erosional susceptibility of bare wet loess surfaces is quite high; therefore, strong erosion processes prevail on the gentle slopes. On the upper region of TR Catchment gully erosion is typical erosion form, which appear not just in arable land with rare vegetation, but it is revealing phenomena under forest coverage as well. This can be the reason, the relatively high SSC concentration from forest. Sub-catchments TR1-TR2-TR6, with low relief contribute relatively little to the instream suspended sediment concentration. Although, orchard and pasture generally have great erosion potential, but in TR Catchment these land use types are located in rather flat areas.

3.4. The link between connectivity descriptors and model parameters

Table 11 gives an overview of the regression functions based on the morphometric catchment descriptors and their coefficients of determination against the calibrated model parameters. All model parameters required at least two descriptors for an optimal regression, and none required more than three. The relative error of the calibrated against the regression value of the parameter was in general smaller for the sub-catchments than for the undivided catchment. However, coefficients of determination were too low for a decisive conclusion.

The independence of the regression model fit to the catchment area implies that equally good parameter estimations may be derived irrespective of (sub) catchment size. This means that hydrological connectivity, in its different descriptors, is equally well represented in the lumped catchment configuration as in the spatially differentiated configuration.

Table 11: Regression functions and their coefficients of determination for the model parameters.

<i>Model parameter</i>	<i>function</i>	<i>R²</i>
PERSiST		
flow_”a”	$H_{range}^{9.7} \cdot IC^{-21.8}$	0.99
flow_”b”	$0.73 - 0.14 \cdot rA_{agri} - 3.63 \cdot 10^{-6} \cdot L_{av} - 8.05 \cdot 10^{-10} \cdot A$	1.00
snow multiplier	$-1.10 + 1.37 \cdot 10^{-2} \cdot H_{max} - 1.21 \cdot 10^{-1} \cdot IC - 4.48 \cdot 10^{-4} \cdot R_{min}$	0.99
INCA-P		
flow_”a”	$2.94 - 5.78 \cdot 10^{-9} \cdot A - 0.17 \cdot IC$	0.98
flow_”b”	$4.98 \cdot 10^{-2} + 7.69 \cdot 10^{-6} \cdot L_{max} + 7.69 \cdot 10^{-6} \cdot H_{range}$	0.98
Base Flow Index	$-8.45 \cdot 10^{-1} + 3.61 \cdot 10^{-1} \cdot K_G + 3.53 \cdot 10^{-3} \cdot H_{av} + 3.46 \cdot 10^2 \cdot DD$	0.97
groundwater zone time constant	$1.02 \cdot 10^2 - 2.86 \cdot 10^{-2} \cdot R_{min} - 3.36 \cdot 10^1 \cdot K_G + 3.20 \cdot 10^{-2} \cdot L_{max}$	1.00
max. groundwater effective depth	$2.44 \cdot 10^2 - 1.86 \cdot 10^{-1} \cdot H_{max} - 5.21 \cdot 10^{-1} \cdot H_{min} + 1.24 \cdot 10^{-3} \cdot L_{max}$	1.00



3.5. Results of the scenario analyses

One way to assess the possible changes of future hydrologic conditions and sediment transport processes at catchment scale is to use ensemble of climatic and management scenarios. In this study, we have defined scenarios representing possible changes in catchment scale management. We combine these management and climate scenarios into storylines, which help convey the output of the simulations into quantitative expectations for the future sediment losses in the TR and ER Catchment.

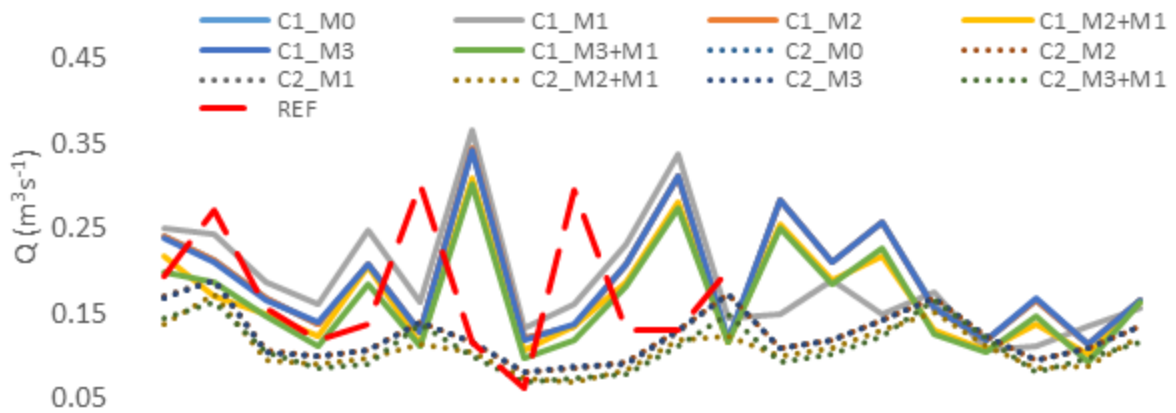
Table 12. The scenario matrix, used to run the catchment-based models

CLIMATE CHANGE SCENARIOS		LAND USE CHANGE SCENARIOS		
Code	Short description	Code	Short description	SLOPE
				above 12% below 12%
C0	present climate	M0	reference (present) land use	NO changes
C1	slightly more rainfall			
C2	much more rainfall			
C0	present climate	M1	whole year soil coverage	Winter cover on all arable land
C1	slightly more rainfall			
C2	much more rainfall			
C0	present climate	M2	deforestation	30% of forest to arable 20% of forest to arable
C1	slightly more rainfall			
C2	much more rainfall			
C0	present climate	M3	afforestation	30% of arable to forest 50% of arable to forest
C1	slightly more rainfall			
C2	much more rainfall			
C0	present climate	M1 + M2	deforestation as in M2 but winter coverage on arable lands	
C1	slightly more rainfall			
C2	much more rainfall			
C0	present climate	M1 + M3	afforestation as in M3 and winter coverage of arable lands	
C1	slightly more rainfall			
C2	much more rainfall			

Figures 15.a-b demonstrate the combined effects of various land use and climate scenarios on water discharge in TR and ER catchments, as simulated by the PERSiST model. The baseline is the present – reference (REF) climate, compared to slight (C1) and drastic (C2) reduction in precipitation amounts. An overview of the scenario matrix is given in Table 12.



a.



b.

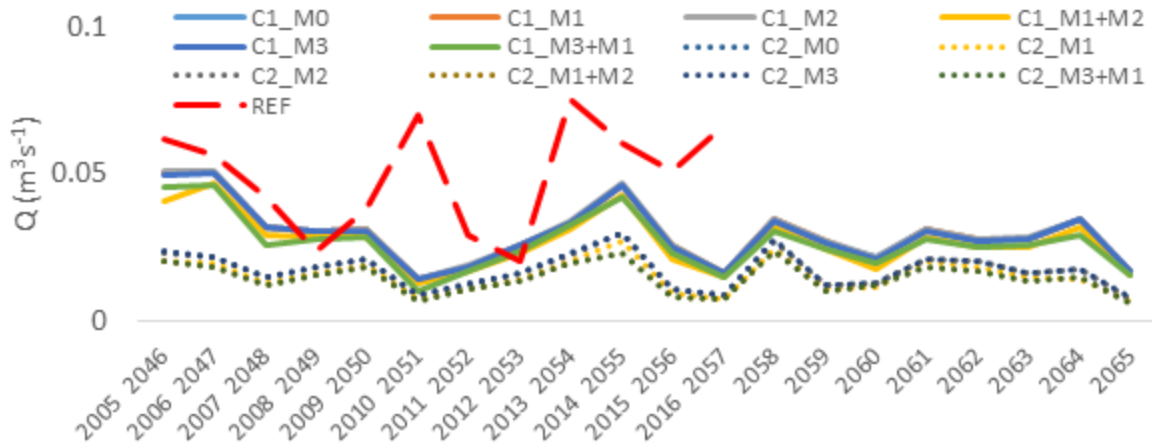


Figure 15. a-b. Simulated impact of the projected climate change and management scenarios on yearly average discharge at the a) TR and b) ER catchment outlets

In Figure 16, we present the relative changes in sediment losses compared to the baseline (present climate and present land use) scenario for the TR and ER catchments.

The main conclusions from the scenario analyses are as follows:

- The discharge is mainly driven by climatic forces. In the ER catchment the management effect is almost not visible compared to the climate effect (Figure 15 b). As for the TR watershed, some slight changes in total runoff can be obtained if applying climate adaptive practices.
- When comparing the effect of various land management options (Figure 16), we can conclude that the soil particle losses will increase in the future if no changes in management will be introduced (M0 shows increase with future climate scenarios). As it was expected, afforestation and winter soil cover can mitigate the effects of extreme weather events but reducing soil losses up from 30 to 40 %

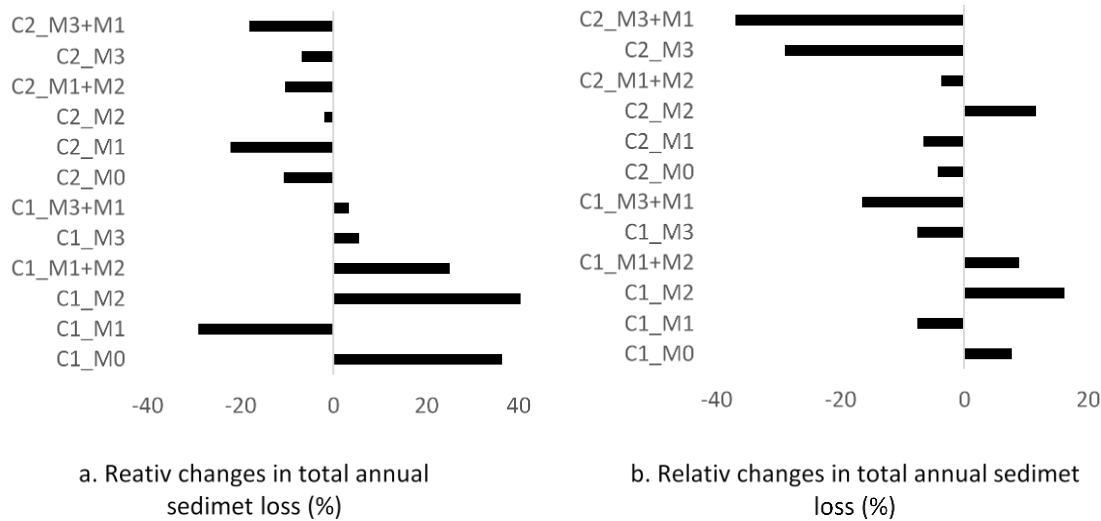


Figure 16. Relative changes in sediment losses for different land management scenarios in reference to present land management for period (2046-2065) in entire TR and ER Catchments

3.6. Recommendations on climate smart solutions for maintaining/improving soil and water quality

From the scenario analyses, performed within the frames of the Project it has clearly been shown, that climate smart solutions are needed for reducing soil loss and increase in suspended sediment concentration in the surface water bodies. This Project was not focusing on other factors, influencing water quality, but we assume, that with increase in soil losses we can expect increase in nutrient losses towards the streams and the lakes.

Our results are in agreement with those, obtained in the REFRESH EU project, aiming to develop adaptation strategies to protect the freshwater ecosystems in Europe. However, that project was strongly focusing on watershed level processes.

As much can be done at field level, soil (reducing erosion risk, improving soil structure and soil water retention etc.) and water protection should be coupled. According to our results land use change is not enough (and might be not realistic either) for mitigating the possible harmful effects of climate change.

Hereby we would like to list some common and innovative solutions, used in other countries that could be considered in the future.

Even though water quantity and quality problems are detected and cause trouble in the surface water bodies, the whole catchment area is contribution to their formation. Thus, the mitigation strategies should be introduced at all the levels possible (Figure 17), also considering land use management aspects.

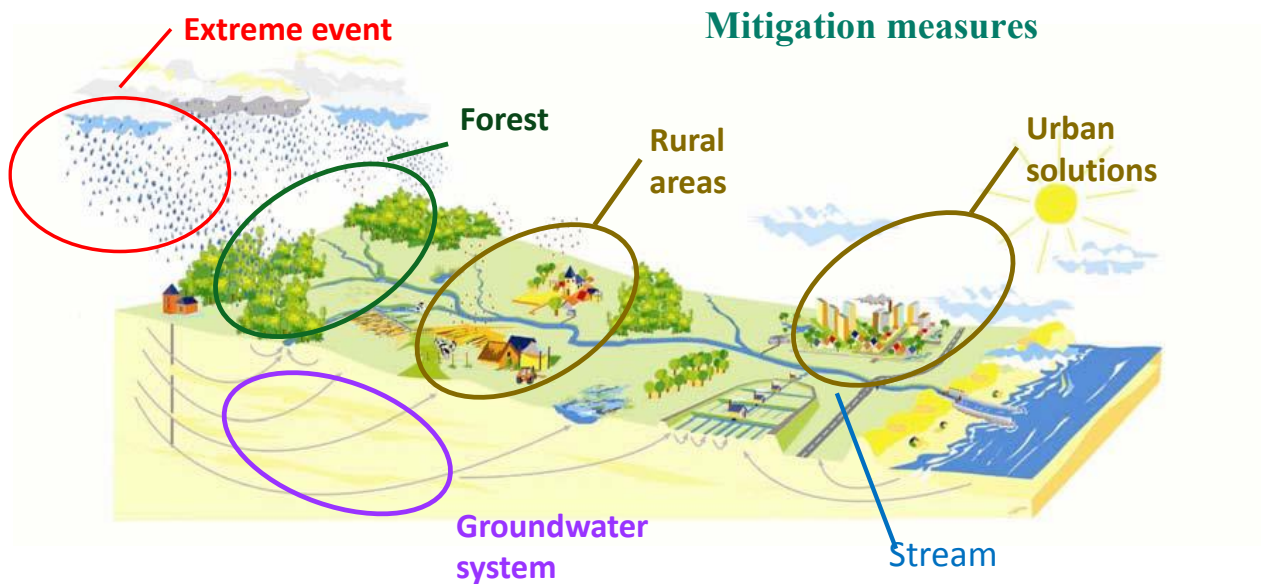


Figure 17. Catchment-based concept of introducing mitigation measures

Example of possible measures to reduce flash floods and soil and nutrient losses:

- Water retention in the forest
- Fertilization planning
- Reduced tilling (shallow cultivation is believed to be one of the best options in Hungary)
- Buffer strips
- Grass covered waterways
- Sedimentation ponds
- Constructed wetlands
- Restauration of streams
- Measures for point sources
- Urban solutions (green roofs; vegetation areas for improving percolation; prolong waterways)

Water retention in the forest:





Measures in the stream



Grass covered waterways





4. Discussion

4.1. The Project's achievements in the light of the expected deliverables

According to the Proposal, the expected practical and scientific impacts of the Project are the followings:

- *providing appropriate background for joint implementation of the Water Framework Directive and Soil Protection Strategy*; we hope that the implementation of the Project i) facilitated the development of a common understanding between researchers, coming from different fields (hydrologists, soil scientists, climatologists, statisticians, modellers etc.); ii) contributed to coupling multi-scale data from both, spatial and temporal aspects as well as to coupling methods (statistical, GIS-based and process-based models) and iii) can provide a background in the future for regarding the catchment and field level processes as a whole system.
- *new, multi-scale soil and hydrological database*; such a working database have been constructed and used during the project.
- *calibrated parameter sets of INCA-SED model for a Hungarian site*; The SWAP model has been applied before for Hungarian sites, but not for the Balaton Watershed, so from this aspect the calibrated SWAP parameters have also value; However, according to the information we have the present study is the first application of the PERSiST and INCA-P models to Hungarian conditions, concluding, that these models area capable to simulate the hydrological and erosion processes in the study region. The calibrated parameter sets can be used in the future to make the model adaptation more simple.
- *extension of theoretical knowledge on processes of flow and sediment transport formation*; Regarding these objectives, we have some publications under preparations on the i) connectivity issues and ii) event-based studies.
- *harmonised at plot and catchment scales adaptation strategies for mitigating the possible harmful effects of climate change and extreme weather events*; This objective could not be fully achieved. Without successful model validation we do not have the right to perform scenario analyses, and the validation of the plot-scale model was not possible in the frames of the project due to several constrains – arising mainly from the difficulties in measuring the soil water content in field conditions. From this aspect we can say, that our modelling efforts contributed to reduce reducing the knowledge gaps in the field of climate-smart adaptation strategies in agricultural and landscape management.



5. List of references

6. ALEXANDER, L.V. 2016. Global observed long-term changes in temperature and precipitation extremes: A review of progress and limitations in IPCC assessments and beyond. *Weather and Climate Extremes*. **11**, 4-16.
7. BALDOCCHI, D.D., XU, L. & KIANG, N. 2004. How plant function-type, weather, seasonal drought, and soil physical properties alter water and energy fluxes of an oak-grass savanna and an annual grassland. *Agricultural and Forest Meteorology*. **123**. 13-39.
8. BRANDT, S.C.J. 1989. The size distribution of throughfall drops under vegetation canopies. *Catena*. **16**. 507–524.
9. CALDER, I.R. 1996. Dependence of raianfall interception on drop size: 1. Development of the two-layer stochastic model. *Journal of Hydrology*. **185**. 363-378.
10. CASTILLO, V.M., GÓMEZ-PLAZA, A. & MARTÍNEZ-MENA, M. 2003. The role of anecedent soil water content in the runoff response of semiarid catchments: a simulation approach. *Journal of Hydrology*. **284**. 114-130.
11. CENTERI, Cs., PATAKI, R. & BARCZI, A. 2001. Soil erosion, soil loss tolerance and sustainability in Hungary. 3rd International Conference on Land Degradation and Meeting of the IUSS Subcomission C – Soil and water Convservation. September 17-21, Rio de Janeiro, Brazil.
12. CENTERI, Cs., AKÁC, A. & JAKAB, G. 2012. Land use change and soil degradation in a nature protected area of East-Central Europe. In: Aubrecht, C., Freire, S., Steinnocher, K. (szerk.) *Land Use: Planning, Regulations, and Environment*. New York: Nova Science Publishers Inc., p. 211–242.
13. CORINE Felszínborítási Adatbázis (CLC50) 2006. Földmérési és Távérzékelési Intézethttp://fish.fomi.hu/letoltes/nyilvanos/corine/clc50_referencia_cikk.pdf
14. CRUZ-MARTINEZ, K., SUTTLE, K.B., BRODIE, E.L., POWER, M.E., ANDERSEN, G.L. & BANFIELD, J.F. 2009. Despite strong seasonal responses, soil microbial consortia are more resilient to longüterm changes in rainfall than overlying grassland. *The ISME Journal*. **3**. 738-744.
15. CSORBA, SZ., FARKAS, Cs. & BIRKÁS, M. 2011. Kétpórusú víztartóképesség-függvény a talajművelés-hatás kimutatásában. *Agrokemia & Talajtan*. **60**. 325–342.
16. DAWSON, 1967. Ionic composition of rain during sixteen convective showers [Atmospheric Environment](#). **12**. 1991–1999.
17. DÖVÉNYI Z. (Szerk.), 2010. Magyarország kistájainak katasztere. MTA Földrajztudományi Kutatóintézet. Budapest.
18. FARKAS, Cs., BELDRING, S., BECHMANN, M. & DEELSTRA, J., 2013. Soil erosion and phosphorus losses under variable land use as simulated by the INCA-P model. *Soil Use and Management*. **29(s1)**. 124–137.
19. FARKAS, Cs., GELYBÓ, Gy., BAKACSI, Zs., HOREL, A., HAGYÓ, A., DOBOR, L., KÁSA, I. & TÓTH, E. 2014. Impact of expected climate change on soil water regime under different vegetation conditions. *Biologia*. **69**. 1510–1519.
20. FAŠKO, P., LAPIN, M. & PECHO, J., 2008. 20-year extraordinary climatic period in Slovakia. *Meteorol. Časopis*. **11**. 99–105.
21. GALLOWAY, J.N., LIKENS, G.E., KEENE W.C. & MILLER, J. M. 1982. The composition of precipitation in remote areas of the world, *J. Geophys. Res.*, **87**. 8771–8786.
22. HOREL, A., LICHNER, L., KODESOVA, R. & STEKAUEROVA, V. 2015a. Effects of land use and irrigation intensity on the transport of iodide in structured clay loam soil. *Agrokemia & Talajtan*. **64**. 391–402.
23. HOREL, A., TÓTH, E., GELYBÓ, Gy., KÁSA, I., BAKACSI, Zs. & FARKAS, Cs. 2015b. Effects of Land Use and Management on Soil Hydraulic Properties. *Open Geosciences*. **1**.742–754.
24. IPCC. 2007. *Climate Change. Impacts, adaptation and vulnerability*. In: Parry M.L., Canziani O.F., Palutikof J.P., van der Linden P.J. & Hanson C.E. (eds), *Contribution of Working Group II to the Fourth Assessment Report of the Intergovernmental Panel on Climate Change*. Cambridge University Press, Cambridge, 976 pp.
25. JAKAB, G.I. 2014. A vonalas erózió Magyarországon. *Talajvédelem*. Szent István Egyetemi Kiadó, Gödöllő, pp. 49–88.
26. JORDÁN, Gy., VAN ROMPAEY, A., SZILASSI, P., CSILLAG, G., MANNAERTS, C. & WOLDAI, T. 2005. Historical land use changes and their impact on sediment fluxes in the Balaton basin (Hungary). *Agriculture, Ecosystems and Environment*. **108**.119–133.



27. KEGGENHOFF, I., ELIZBARASHVILI, M., AMIRI-FARAHANI, A. & KING, L. 2014. Trends in daily temperature and precipitation extremes over Georgia, 1971–2010, *Weather and Climate Extremes*. **4**: 75–85.
28. KERÉNYI A., 1984. A csepperózió hatása a homokszemcsék méret szerinti differenciálódására. *Agrokémia és Talajtan*. **33**. 63–74.
29. KERÉNYI A., 1986. Az iniciális erózió laboratóriumi vizsgálata homokon és szerkezetes talajon. *Agrokémia és Talajtan*. **35**. 18–38.
30. KLEIN TANK A.M.G., KÖNNEN G.P. 2003. Trends in indices of daily temperature and precipitation extremes in Europe, 1946–99 *Journal of Climate* **16**. 3665–3680.
31. LAKATOS, M., SZENTIMREY, T., BIRSZKI, B., KÖVÉR, ZS., BIHARI, Z. & SZALAI, S. 2007. Changes of temperature and precipitation extremes following homogenization. *Acta Silv. Lign. Hung.* **3**. 87–95.
32. LICHNER, L., DUŠEK, J., DEKKER, L. W., ZHUKOVA, N., FAŠKO, P., HOLKO, L. & ŠÍR, M., 2013. Comparison of two methods to assess heterogeneity of water flow in soils. *J. Hydrol. Hydromech.* **61**. 299–304.
33. LIU, H., LEI, T.W., ZHAO, J., YUAN, C.P. & QU, L.Q. 2011. Effects of rainfall intensity and antecedent soil water content on soil infiltrability under rainfall conditions using the run off-on-out method. *Journal of Hydrology*. **396**. 24–32.
34. MEDEIROS, P.H.A., GÜNTNER, A., FRANCKE, T., MAMEDE, G.L., & DE ARAÚJO, J.C. 2010. Modelling spatio-temporal patterns of sediment yield and connectivity in a semi-arid catchment with the WASA-SED model, *Hydrological Sciences Journal*. **55**. 636–648.
35. MOHAMMAD, A.G. & ADAM, A.A., 2010. The impact of vegetative cover type on runoff and soil erosion under different land uses. *Catena*. **81**. 97–103.
36. MOORE, I.D. 1983. Throughfall pH: effect of precipitation timing and amount. *Water Resources Bulletin*. **19**. 961–965.
37. MORGAN, R.P.C., 1978. Field studies of rainsplash erosion. *Earth Surface Processes*. **3**. 295–299.
38. MORGAN, R.P.C. & DUZANT, J.H. 2008. Modified MMF (Morgan-Morgan-Finney) model for evaluating effects of crops and vegetation cover on soil erosion. *Earth Surface Processes and Landforms*. **32**. 90–106.
39. MÜLLER, K., STENGER, R. & RAHMAN, A. 2006. Herbicide loss in surface runoff from a pastoral hillslope in the Pukemanga catchment (New Zealand): Role of pre-event soil water content. *Agriculture, Ecosystems and Environment*. **112**. 381–390.
40. NANKO, K., HOTTA, N. & SUZUKI, M. 2006. Evaluating the influence of canopy species and meteorological factors on throughfall drop size distribution. *Journal of Hydrology*. **329**. 422–431.
41. NGUYEN, H.L., LEERMAKERS, M., OSÁN, J., TÖRÖK, S. & BAEYENS, W. 2005. Heavy metals in Lake Balaton: water column, suspended matter, sediment and biota. *Science of the Total Environment*. **340**. 213–230.
42. PENMAN, H.L. 1948. Evaporation from open water, bare soil and grass. *Proceedings of the Royal Society of London. Series A, Mathematical and Physical Sciences*. **193**. 120–145.
43. PILCH, M. & ERDMAN, C.A., 1987. Use of breakup time data and velocity history data to predict the maximum size of stable fragments for acceleration-induced breakup of liquid drop. *International Journal of Multiphase Flow*. **13**. 741–757.
44. RAJKAI K., 1988. A talaj víztartóképesége és egyéb tulajdonságok összefüggésének vizsgálata. *Agrokémia és Talajtan*. 36–37. 15–30.
45. Rajkai K., 2012. Talajfizika. *Agrokémia és Talajtan*. 65. Supplementum, 47–92.
46. Rügner, H., Schwientek, M., Beckingham, B., Kuch, B. & Grathwohl, P. 2013. Turbidity as a proxy for total suspended solids (TSS) and particle facilitated pollutant transport in catchments. *Environmental Earth Sciences*. **69**. 373–380.
47. Surda, P., Lichner, L., Nagy, V., Kollar, J., Iovino, M. & Horel, A. 2015. Effects of vegetation at different succession stages on soil properties and water flow in sandy soil. *Biologia*, **70**. 1–6.
48. Szilassi, P., Jordan, Gy., van Rompaey, A. & Csillag, G., 2006. Impacts of historical land use changes on erosion and agricultural soil properties in the Kali Basin at Lake Balaton, Hungary. *Catena*. **68**. 96–108.
49. Thurow, T. L. Blackburn, W. H. Warren, S. D. & Taylor, C. A. 1987. Rainfall Interception by Midgrass, Shortgrass, and Live Oak Mottes *Journal of Range Management*. **40**. 455–460.
50. Zanchi, C. & Torri, D., 1980. Evaluation of rainfall energy in Central Italy. In: De Boodt, M., Gabriels, D. (eds). *Assessment of erosion*. Wiley, Chichester, pp. 133–142.



51. Ziadat, F. M. & Taimeh, A. Y., 2013. Effect of rainfall intensity, slope, land use and antecedent soil moisture on soil erosion in an arid environment. *Land Degradation & Development*. 24. 582–590.
52. Young RA, Mutchler CK (1969a). Effect of slope shape on erosion and runoff. *Transactions of the American Society of Agricultural Engineers* 12: 231-233.
53. Wischmeier WH, Smith DD (1978). Predicting rainfall erosion losses. A guide to conservation planning. *USDA Agricultural Handbook 537*, Washington, DC, pp. 58.
54. Liu BY, Nearing MA, Risse LM (1994). Slope gradient effects on soil loss for steep slopes. *Transactions of the American Society of Agricultural Engineers* 37: 1835-1840.
55. Gabriels D (1999). The effect of slope length on the amount and size distribution of eroded silt loam soils: short slope laboratory experiments on interrill erosion. *Geomorphology* 28: 169-172
56. Chaplot VAM, Le Bissonnais Y (2003). Runoff features for interrill erosion at different rainfall intensities, slope lengths, and gradients, in an agricultural loessial hillslope. *Soil Science Society of America Journal* 67: 844-851. <https://www.ipcc.ch/ipccreports/tar/wg1/029.htm>
57. Baartman, JEM, Masselink, R, Keesstra, SD, Temme, AJAM. 2013. Linking landscape morphological complexity and sediment connectivity. *Earth Surface Processes and Landforms* 38: 1457-1471. DOI: 10.1002/esp.3434
58. Bracken, LJ, Croke, J. 2007. The concept of hydrological connectivity and its contribution to understanding runoff-dominated geomorphic systems. *Hydrological Processes* 21: 1749-1763. DOI: <http://dx.doi.org/10.1002/hyp.6313>
59. Cammeraat, LH. 2002. A review of two strongly contrasting geomorphological systems within the context of scale. *Earth Surface Processes and Landforms* 27: 1201-1222. DOI: 10.1002/esp.421
60. Döll, P, Kaspar, F, Lehner, B. 2003. A global hydrological model for deriving water availability indicators: model tuning and validation. *Journal of Hydrology* 270: 105-134. DOI: [http://dx.doi.org/10.1016/S0022-1694\(02\)00283-4](http://dx.doi.org/10.1016/S0022-1694(02)00283-4)
61. Grayson, RB, Blöschl, G, Moore, ID. 1995. Distributed parameter hydrologic modelling using vector elevation data: Thales and TAPES-C In *Computer Models of Watershed Hydrology*, Singh, VP (ed). Water Resources Publisher: Highlands Ranch, Colorado, USA; 669-695.
62. Hardy, RJ, Bates, PD, Anderson, MG. 1999. The importance of spatial resolution in hydraulic models for floodplain environments. *Journal of Hydrology* 216: 124-136. DOI: [http://dx.doi.org/10.1016/S0022-1694\(99\)00002-5](http://dx.doi.org/10.1016/S0022-1694(99)00002-5)
63. Hooke, J. 2003. Coarse sediment connectivity in river channel systems: a conceptual framework and methodology. *Geomorphology* 56: 79-94. DOI: [http://dx.doi.org/10.1016/S0169-555X\(03\)00047-3](http://dx.doi.org/10.1016/S0169-555X(03)00047-3)
64. Krysanova, V, Müller-Wohlfeil, D-I, Becker, A. 1998. Development and test of a spatially distributed hydrological/water quality model for mesoscale watersheds. *Ecological Modelling* 106: 261-289. DOI: [http://dx.doi.org/10.1016/S0304-3800\(97\)00204-4](http://dx.doi.org/10.1016/S0304-3800(97)00204-4)
65. Maidment, DR. 1996. GIS and hydrologic modeling—an assessment of progress. In *Proceedings of the Third International Conference on Integrating GIS and Environmental Modelling*. National Center for Geographical Information and Analysis: Santa Barbara, CA, USA.
66. Marchamalo, M, Hooke, JM, Sandercock, PJ. 2016. Flow and Sediment Connectivity in Semi-arid Landscapes in SE Spain: Patterns and Controls. *Land Degradation & Development* 27: 1032-1044. DOI: 10.1002/ldr.2352
67. Masselink, RJH, Keesstra, SD, Temme, AJAM, Seeger, M, Giménez, R, Casali, J. 2016. Modelling discharge and sediment yield at catchment scale using connectivity components. *Land Degradation & Development* 27: 933-945. DOI: 10.1002/ldr.2512
68. McDonnell, JJ, Sivapalan, M, Vaché, K, Dunn, S, Grant, G, Haggerty, R, Hinz, C, Hooper, R, Kirchner, J, Roderick, ML, Selker, J, Weiler, M. 2007. Moving beyond heterogeneity and process complexity: A new vision for watershed hydrology. *Water Resources Research* 43: n/a-n/a. DOI: 10.1029/2006WR005467
69. Medeiros, P, Güntner, A, Francke, T, Mamede, G, de Araújo, J. 2010. Modelling spatio-temporal patterns of sediment yield and connectivity in a semi-arid catchment with the WASA-SED model. *Hydrol. Sci. J* 55: 636-648
70. Mueller, EN, Wainwright, J, Parsons, AJ. 2007. Impact of connectivity on the modeling of overland flow within semiarid shrubland environments. *Water Resources Research* 43: n/a-n/a. DOI: 10.1029/2006WR005006
71. New, M, Lister, D, Hulme, M, Makin, I. 2002. A high-resolution data set of surface climate over global land areas. *Climate Research* 21: 1-25



72. Taylor, PD, Fahrig, L, Henein, K, Merriam, G. 1993. Connectivity is a vital element of landscape structure. *Oikos* 68: 571-573. DOI: <http://dx.doi.org/10.2307/3544927>
73. Western, AW, Blöschl, G, Grayson, RB. 2001. Toward capturing hydrologically significant connectivity in spatial patterns. *Water Resources Research* 37: 83-97. DOI: 10.1029/2000WR900241
74. Kirkby, M. J., Irvine, B. J., Jones, R. J. A., Govers, G. and PESERA team (2008), The PESERA coarse scale erosion model for Europe. I. – Model rationale and implementation. *European Journal of Soil Science*, 59: 1293–1306. doi:10.1111/j.1365-2389.2008.01072.x Arnold, J. G., Srinivasan, R., Muttiah, R. S., & Williams, J. R. (1998). Large area hydrologic modeling and assessment part I: model development. *Journal of the American Water Resources Association*. <http://doi.org/10.1111/j.1752-1688.1998.tb05961.x>
75. Beven, K. and Freer, J. (2001), A dynamic TOPMODEL. *Hydrol. Process.*, 15: 1993–2011. doi:10.1002/hyp.252
76. Borselli, L., Cassi, P., & Torri, D. (2008). Prolegomena to sediment and flow connectivity in the landscape: A GIS and field numerical assessment. *Catena*, 75(3), 268–277. <http://doi.org/10.1016/j.catena.2008.07.006>
77. Bossa, A. Y., & Diekkrüger, B. (2012). Estimating scale effects of catchment properties on modeling soil and water degradation in Benin (West Africa). *iEMSs 2012 - Managing Resources of a Limited Planet: Proceedings of the 6th Biennial Meeting of the International Environmental Modelling and Software Society*, 2974–2981.
78. Ducharne, a. (2009). Reducing scale dependence in TOPMODEL using a dimensionless topographic index. *Hydrology and Earth System Sciences*, 13(12), 2399–2412. <http://doi.org/10.5194/hess-13-2399-2009>
79. Horritt, M. S., & Bates, P. D. (2001). Effects of spatial resolution on a raster based model of flood flow. *Journal of Hydrology*, 253(1–4), 239–249. [http://doi.org/10.1016/S0022-1694\(01\)00490-5](http://doi.org/10.1016/S0022-1694(01)00490-5)
80. Shrestha, R., Tachikawa, Y., & Takara, K. (2006). Input data resolution analysis for distributed hydrological modeling. *Journal of Hydrology*, 319(1–4), 36–50. <http://doi.org/10.1016/j.jhydrol.2005.04.025>
81. Thomas, J., & Prasannakumar, V. (2015). Comparison of basin morphometry derived from topographic maps, ASTER and SRTM DEMs: an example from Kerala, India. *Geocarto International*, 30(3), 346–364. <http://doi.org/10.1080/10106049.2014.955063>
82. Valeo, C., & Moin, S. M. A. (2000). Grid-resolution effects on a model for integrating urban and rural areas. *Hydrological Processes*, 14(14), 2505–2525. [http://doi.org/10.1002/1099-1085\(20001015\)14:14<2505::AID-HYP111>3.0.CO;2-3](http://doi.org/10.1002/1099-1085(20001015)14:14<2505::AID-HYP111>3.0.CO;2-3)
83. Wolock, M., & Survey, U. S. G. (1997). Effects of subbasin size on topographic characteristics and, 31(8), 1989–1997.
84. Zhang, W., & Montgomery, D. R. (1994). Digital elevation model grid size, landscape representation. *Water Resour. Res*, 30(4), 101.
85. Semenov MA, Barrow EM (2002) LARS-WG: a stochastic weather generator for use in climate impact studies, 28 p